The Identification of Distinct Patterns in California Temperature Trends

by

Eugene C. Cordero and Wittaya Kessomkiat
Department of Meteorology
San José State University, San José, CA 95192-0104

John Abatzoglou
Department of Geography
University of Idaho, Moscow, ID 83844-3021

Steven A. Mauget
U.S. Department of Agriculture-Agricultural Research Service
USDA Plant Stress and Water Conservation Laboratory, Lubbock, TX 79415

Submitted to
Climatic Change
August 28, 2009
Accepted
November 4, 2010

Corresponding Author:

Dr. Eugene Cordero
Department of Meteorology
San José State University
San José, CA 95192-0104
408 924-5188 (office)
408 924-5191 (fax)
cordero@met.sjsu.edu

Abstract

Regional changes in California surface temperatures over the last 80 years are analyzed using station data from the US Historical Climate Network and the National Weather Service Cooperative Network. Statistical analyses using annual and seasonal temperature data over the last 80 years show distinctly different spatial and temporal patterns in trends of maximum temperature (Tmax) compared to trends of minimum temperature (Tmin). For trends computed between 1918 and 2006, the rate of warming in Tmin is greater than that of Tmax. Trends computed since 1970 show an amplified warming rate compared to trends computed from 1918, and the rate of warming is comparable between Tmin and Tmax. This is especially true in the southern deserts, where warming trends during spring (March-May) are exceptionally large. While observations show coherent statewide positive trends in Tmin, trends in Tmax vary on finer spatial and temporal scales. Accompanying the observed statewide warming from 1970 to 2006, regional cooling trends in Tmax are observed during winter and summer. These signatures of regional temperature change suggest that a collection of different forcing mechanisms or feedback processes must be present to produce these responses.

KEYWORDS: Atmospheric science, California temperature, statistical analysis, air temperature, observations

1 Introduction

Global average surface temperatures have increased +0.74°C ± 0.18°C between 1906–2005 (e.g., IPCC 2007). Variations in interannual to multi-decadal temperatures are important to understand as they provide clues about the relationship between different forcing mechanisms (e.g., Cordero and Forster 2006). Observations suggest an acceleration in the rate of warming of global average surface temperatures over the twentieth century, with the trend over the last 50 years of the twentieth century (+0.13°C ± 0.03°C dec^{-1}) being nearly twice the magnitude of the first 50 years (+0.07°C ± 0.03°C dec^{-1}), with an even greater warming rate observed for the last 25 years (+0.18°C± 0.05°C dec^{-1}). While various forcing mechanisms have been identified, increasing greenhouse gas concentrations appear to be primarily responsible for this enhanced global-scale warming (IPCC 2007).

There have also been differences in the trend of minimum temperatures (Tmin) and maximum temperatures (Tmax). Vose et al. (2005) found that the global Tmin increased more rapidly than the global Tmax (+0.20°C dec^{-1} vs. +0.14°C dec^{-1}) during 1950–2004, although from 1979–2004, global Tmin and Tmax increased at nearly the same rate (+0.29°C dec^{-1}). Various forcing agents have been suggested for observed differential warming rates of Tmin and Tmax including the role of urbanization and land-use change (Bonan 2001; Kalnay and Cai 2003), and regional aerosol loading (Wild et al. 2007). Resolving differences between the time varying trends in Tmin and Tmax is critical in uncovering the source of recent temperature trends and improving projections of future climate change.

In addition to both time varying and diurnal asymmetries in temperature trends, spatial differences in temperature trends have been observed. For example, over the continental U.S., Lund et al. (2001) found annual warming trends in the Northeast, Northern Midwest, and West Coast, but cooling trends in the Southeast. Components of these warming trends have been

attributed to changes in land-surface feedback processes (e.g., Yang et al. 2001) and large-scale climate dynamics (e.g., Abatzoglou and Redmond 2007), while the cooling in the Southeast has been attributed to high aerosol levels associated with regional energy and industrial production (Saxena and Yu 1998).

Most studies have focused on large-scale temperature trends; however, advancing our understanding of temperature changes at finer spatial scales represents a pressing scientific question needed in climate change assessment. The state of California is a suitable test-bed for examining regional and local temperature trends given the complex physical controls on regional climate across the state. Furthermore, as California's ecology and economy appear sensitive to changes in climate (Hayhoe et al. 2004), analysis and understanding of observed trends is important for refining future climate projections for climate sensitive sectors and natural resources within the state.

A number of prior studies have examined California temperature trends from statewide to local levels. LaDochy et al. (2007) analyzed surface station data in California from 1950–2000 and found greater warming in Tmin compared to Tmax for most regions in California and concluded that warming trends were most pronounced in urban areas due to the influence of the urban heat island effect. Christy et al. (2006) suggested that warming in Tmin over the Central Valley during summer, and a lack of warming at the higher elevation stations in the Sierra Nevada, were primarily due to the influence of irrigation. Later studies by Bonfils et al. (2006) and Bonfils and Lobell (2007) found that trends in the Central Valley were due to *both* irrigation and anthropogenic greenhouse gases (GHGs). Lebassi et al. (2009) found summertime Tmax cooling trends near the coast over the last 30 years in the Los Angeles and San Francisco basins. Their analysis suggested that these cooling trends were a result of an enhanced sea breeze circulation driven by warming over the interior. Understanding how various forcings (both

natural and anthropogenic) affect California's climate remains an area of active research (e.g., Bonfils et al. 2008).

While it is clear that temperatures across California are changing, several outstanding questions remain. How have temperatures changed across California and are there distinct regional signatures in those changes? In addition, are trends in Tmin and Tmax different, and what do these trends tell us about the possible forcing agents? This study aims to address these questions by applying analytical techniques to investigate the spatial and temporal structure of California surface temperature trends using two different datasets. The study also suggests that some of these analytical techniques could serve as valuable diagnostics for model attribution studies.

2 Data and methodology

Monthly temperature observations from the US Historical Climate Network (USHCN) (USHCN urban heat-adjusted, Williams et al. 2007) and the daily temperature observations from National Weather Service Cooperative Network (COOP) network were obtained from the National Climatic Data Center (NCDC). Observations from 58 USHCN stations (54 California stations and 4 additional USHCN stations from neighboring states) spanning the period 1918–2006 and 272 COOP stations (in California) spanning the period 1950–2006 provide coverage across the state as shown in Figures 1 and 2. While the USHCN is a high quality dataset that includes adjustments for changes in station location and urbanization, the COOP network provides a more detailed view due to a greater density of stations. However, uncertainties in COOP data exist since the data are prone to climate inhomogeneities (e.g., changes in observational methods and/or location) and periods of missing or incomplete data.

Seasonal and annual averages for each dataset were computed using data completeness assurance methods described in Stafford et al. (2000) and Vose et al. (2005). For daily COOP

station data, no month was used if more than six days in the month were missing daily data and no COOP station was used if more than 20% of data were missing during the entire time period or more than four years of data in a decade were missing. Also, for both datasets, no three-month seasons were used if a single month was missing and no year was used if more than one month was missing. While we acknowledge the potential for biases when using station data (e.g., Peterson 2003), these data completeness assurance measures help minimize misinterpretation.

Statewide and regional average temperature trends were computed for each of the datasets. For regional trends, we used an 11 region partitioning of California (see Figure 4) based on patterns of co-variability using monthly temperature and precipitation data from COOP stations (Abatzoglou et al. 2009). Regional temperature trends were computed by averaging all of the stations for each of the 11 defined climate regions, as well as the northern and southern portions of the state delineated by the 36°N parallel following NCDC. For spatial averages, monthly data were reported as missing if more than 50% of the stations failed to report a monthly mean.

Monthly Tmin and Tmax were analyzed in this study. Seasonal and annual averages were calculated using monthly averages, where seasons were defined using standard meteorological definitions of winter (DJF), spring (MAM), summer (JJA), and fall (SON). For Tmin and Tmax, monthly, seasonal, and annual trends were computed using a linear least-square regression for two time periods: 1918–2006 (USHCN data only), and 1970–2006 (USHCN and COOP data). The start of the first time period (1918) corresponds to the period when a significant number of stations have continuous records. The start of the second time period (1970) broadly corresponds to a period of recent warming globally (IPCC 2007). Statistical significance in the trends was determined by computing the standard error of the trend estimate, where temporal autocorrelation is taken into account by adjusting the degrees of freedom, as described in Santer

(2000). Hereafter, statistically significant trends at the 95% confidence level are referred to as warming (positive) and cooling (negative), whereas trends identified as positive or negative are simply the sign of the trend.

2.1 Mann-Whitney Z analysis method

California temperature time series were evaluated using the running Mann-Whitney Z (MWZ) analysis method of Mauget (2003a, b). This approach ranks a time series' data values, samples those rankings over moving time windows of fixed duration (N_s), then converts each sample of rankings into a Mann-Whitney U (MWU) statistic. At a fixed sample size, randomly sampled MWU statistics are normally distributed and proportional to the incidence of high rankings in the sample (Mendenhall et al. 1990; Wilks 1995). Thus, the MWU statistics from sequences of a time series' ranked values can be normalized into MWZ statistics using the parameters of an appropriate MWU null distribution. Using the Monte-Carlo generated MWU null distributions described in Mauget (2003a), temperature rankings with significant positive (negative) MWZ values show a significant incidence of warm (cool) years in a sample relative to a null hypothesis that assumes a stationary climate. Thus the significant MWZ statistics from moving time windows can identify warm and cool periods of N_s years' duration in a temperature data record. To identify temperature regimes of more arbitrary length this process is repeated using sampling windows of N_s = 6–30 years, and the running MWU statistics from each of those 25 analyses are normalized into MWZ statistics by null parameters appropriate for each sample size. The positive and negative MWZ statistics from all 25 tests that exceed a two-sided 95% confidence threshold are then pooled and ordered according to the absolute value of their significance. Finally, the periods resulting in the greatest absolute significance over non-overlapping time windows are identified.

The running MWZ method is robust because it avoids limiting assumptions about how climate varies throughout time. Climate data is frequently subjected to trend analysis, but may not be suitable when climate variation is clearly non-linear. Both Fourier and wavelet analyses can identify non-linear cyclic behavior in a time series, but assumes that climate varies in an idealized cyclic manner. The running MWZ approach makes less-limiting assumptions about how low frequency climate variability occurs; specifically, that such variation consists of non-cyclic intra-to-multi-decadal (IMD) temperature regimes of arbitrary onset and duration. Because of this assumption's generality, the method can detect a wide range of climate variability. A simple positive linear trend in temperature in a time series might be marked by a significant negative MWZ period at the series' beginning, and a significant positive period at the end. A significant warm period immediately preceded by a cool period would show a more abrupt climate shift. Cyclic regimes might be seen in alternating periods of significant high- and low-ranked annual temperature. Given a shading scheme for significance, the simplicity of the method's results – a time series' most significant non-overlapping ranking sequences – makes it possible to graphically identify consistent patterns of IMD temperature variation in groups of time series. One limitation of this method is that complete time series are required for the ranking algorithm. Thus, for using the MWZ method on the USHCN climate data of California, we focus our analysis on the 52 USHCN stations (out of 58) that have continuous records between 1918–2006.

3 Statewide California temperature trends using USHCN data

Time series of annual California Tmin and Tmax temperatures from USHCN data between 1918–2006 are shown in Figure 3. Annual temperature trends showed statistically significant warming (95% confidence level) for both Tmin and Tmax, but with a much larger warming in Tmin (+0.17°C dec^{-1}) compared to Tmax (+0.07°C dec^{-1}). Despite significant

differences in long-term trends, annual Tmin and Tmax were significantly correlated (r=0.61), suggesting the influence of common forcing mechanisms.

4 Regional temperature trends using USHCN data

4.1 Annual analysis: 1918–2006

While distinct warming trends were observed for the state, a more detailed investigation was conducted by spatially stratifying the trends. Annual temperature trends computed for the 1918–2006 period for each of the 11 defined climate regions using USHCN data are shown in Figure 4. For Tmin, annual trends for each region showed warming (statistically significant at the 95% confidence level), with the largest warming found in parts of the Central Valley and Southern California (i.e., Sacramento-Delta (+0.26ºC dec^{-1}), South Interior (+0.22ºC dec^{-1})) and the weakest significant warming found in the Sierras (+0.06ºC dec^{-1}) and the Mojave Desert (+0.09ºC dec^{-1}). For Tmax, 7 out of 11 regions exhibited warming in the annual mean, with the strongest warming found in the Sacramento-Delta (+0.17ºC dec^{-1}) and southern part of the state (+0.10 to +0.16ºC dec^{-1}).

4.2 Comparison of annual trends: 1918–2006 with 1970–2006

It is understood that forcings (i.e., natural and anthropogenic) may interact in a nonlinear fashion, thus affecting temperatures across different time and spatial scales. To evaluate this, we compared annual trends across different regions for two different time periods, 1918–2006 and 1970–2006. The most prominent feature in this comparison (Figure 5) was accelerated warming trends from 1970–2006. Statewide Tmax trends between 1970–2006 (+0.27°C dec^{-1}) were more than three times as large as the trend between 1918–2006 (+0.07°C dec^{-1}), while Tmin trends between 1970–2006 (+0.31°C dec^{-1}) were almost twice as large as trends between 1918–2006 (+0.17°C dec^{-1}). The finding that trends for Tmin were larger than Tmax for the entire period,

while trends in Tmin were nearly the same as Tmax since 1970 is qualitatively similar to results observed for global temperature (Vose et al. 2005).

Although statewide trends in temperature for Tmin and Tmax were about the same since 1970, there were distinct regional differences. In the northern part of the state (North Coast, North Central, and Northeast regions), the average Tmax trend was +0.20°C dec^{-1} while the average Tmin trend was +0.27°C dec^{-1}. In the southern part of the state (South Interior, Mojave Desert and Sonoran Desert regions), the average Tmax trend was +0.41°C dec^{-1} while the average Tmin trend was +0.37°C dec^{-1}. The difference in warming trends between these northern and southern regions was statistically significant and most pronounced in Tmax. Additionally, since 1970, warming Tmin trends were statistically significant in 10 out of 11 regions, while warming Tmax trends were statistically significant in only 6 out of 11 regions. Regions that did not observe a statistically significant warming of Tmax included both coastal (North Coast, Central Coast, and South Coast) and montane (Northeast and Sierra) regions of the state.

4.3 Mann-Whitney Z analysis of annual temperatures

To further explore the timing and duration of annual temperature change in California, Mann-Whitney U statistics were used to identify significant warm and cool periods during 1918–2006 for the USHCN stations. Figures 3 and 6 show the results of this analysis for both Tmin and Tmax, where significant sequences of low- and high-ranked annual temperatures are indicated at 90%, 95%, and 99% confidence levels by blue or red shaded bars.

In Figure 3, the original statewide time series and accompanying MWU statistics are shown together for Tmax and Tmin. For Tmax, cool periods were identified around 1920 and then between the 1940s and the mid-1970s, while a warm period was found after 1986. In contrast, for Tmin there were cool periods between the 1920s and the 1950s, and a warm period after the mid-1970s. In the case of Tmin, the patterns of warm and cold years followed a

somewhat linear increase in temperatures as seen in the time series. However Tmax temperatures were quite different, with two distinct cold periods accompanied by a warmer recent period. Note that in the case of Tmax, a number of warm years around 1960 were embedded within a 30-year cool period. Since the MWZ method identifies maximum Z values for periods between 6-30 years, in this case the 30-year cool period was more significant than the individual cool periods before or after 1960. This analysis also highlights how the use of linear least-squares regression is insufficient to capture the highly non-linear changes observed in temperature, while the MWZ method, which quantifies both the timing and duration of decadal-scale warm and cold periods, is clearly an improved method of characterizing California temperature variability.

Running MWZ statistics were calculated for each of the USHCN stations for Tmax and Tmin and are shown in Figure 6. For Tmax (Figure 6a), there appear to be two periods when a series of warm calendar years were recorded. The first was during ~1925–1942, when approximately 50% of all stations in California experienced a warm Tmax regime, particularly in the northern part of the state. The second warm period was between ~1985–2006, when approximately 80% of all stations experienced a warm Tmax regime. Cool Tmax regimes were generally found between 1945–1975, but the start and end years of those regimes differ between the stations. In addition, about 50% of the stations showed cool Tmax periods early in the record (1918–1925). For Tmin (Figure 6b), over 80% of the stations showed significant cool periods between 1918–1958, and over 85% of the stations showed warm periods between 1978–2006.

4.5 Seasonal and regional analysis: 1918-2006 and 1970-2006

Seasonal trends at the statewide and regional level were analyzed to better understand the results from the annual analysis. Tables 1 and 2 provide the statewide and regional Tmax and Tmin trends for each season using the USHCN data for the period of 1918–2006 and 1970–2006.

In the period since 1918 (Table 1), the statewide seasonal trends were only statistically significant for Tmin and range from +0.14°C dec^{-1} (DJF) to +0.21°C dec^{-1} (JJA). In the period since 1970 (Table 2), the statewide seasonal trends were larger in magnitude, but again only significant for Tmin and during MAM (+0.40°C dec^{-1}) and JJA (+0.32°C dec^{-1}).

At the regional level, Tmax trends were primarily statistically significant in the southern part of the state. From 1970–2006 (Table 2), the largest warming in Tmax occurred in MAM in the southern part of the state, whereas statistically significant warming was identified in relatively few regions apart from the southern interior regions (South Interior, Mojave Desert, and Sonoran Desert) during MAM (+0.61°C dec^{-1}), JJA (+0.41°C dec^{-1}), and SON (+0.46°C dec^{-1}). For Tmin, the strongest warming trends occurred during MAM and were largest in the southern part of the state. While statewide trends during MAM (+0.40°C dec^{-1}) were at least 25% larger than any other season, the largest regional trends were found in the southern interior regions during MAM (+0.54°C dec^{-1}), although relatively strong warming (+0.3 to +0.4°C dec^{-1}) was also apparent during the other seasons in this region. The trend towards a warmer spring in California has also been noted in other studies (e.g., Cayan et al. 2008). In contrast, the majority of regional trends during DJF were not significant for either Tmin or Tmax trends.

This seasonal analysis offers distinct signatures of the regional climate that may offer clues as to the source of these changes. In California, by far the largest warming between 1970-2006 occurred in the southern part of the state (i.e., South Interior, Mojave Desert, and Sonoran Desert regions) during MAM for both Tmin and Tmax trends. Since the rate of warming for Tmax and Tmin are roughly equal (between 1970-2006 in the southern part of the state), this suggests a forcing mechanism (or combination of forcing mechanisms) that affects both minimum and maximum temperatures equally.

5. Individual station trends using USHCN and COOP data

5.1 Temperature trends: annual and seasonal comparison

While averaging station data over a geographical region can provide good estimates for regional trends, it can also obscure finer-scale features. In the following analysis, we examined individual USHCN and COOP station data to determine trends observed at point locations across the state. In Figure 7, annual Tmax and Tmin temperature trends (statistically significant at the 95% confidence level) computed between 1918–2006 are shown for each of the USHCN stations. Not surprisingly, trends calculated at the station level are broadly consistent with trends calculated at the regional level. Most of the individual trends are between +0.16 and +0.33°C dec^{-1} although values exceeding +0.5°C dec^{-1} are seen for Tmin. Moreover, about half of the stations reported statistically significant warming trends for annual Tmax, and three-quarters reported statistically significant warming for annual Tmin (Figure 8a). The larger percentage of warming stations in Tmin compared to Tmax was a consistent feature for all seasons.

Maps of statistically significant annual Tmin and Tmax trends computed between 1970–2006 for the USHCN and the COOP network are shown in Figures 9 and 10. For Tmin, nearly all statistically significant stations warmed (all statistically significant USHCN stations warmed, while only one COOP station exhibited cooling). However, for Tmax there were some stations that showed cooling. In the USHCN network for Tmax, only one station showed cooling, whereas about 8% of stations in the COOP network showed cooling (see Figures 8c and 10). These cooling stations in the COOP data were primarily coastal locations, defined as being located within 45km from the Pacific, and illustrate that the higher spatial resolution of the COOP data may resolve features that are not captured in the coarser USHCN data.

Additional insights into the difference between Tmin and Tmax trends in the period after 1970 were found by examining the seasonal variations in the trends. In the USHCN and COOP

Tmin trends, warming was widespread during MAM, JJA, and SON (35-60% of the stations), and comparably less ubiquitous in DJF (20% of stations; see Figures 8b and 8c). As regional variations in the magnitude and sign of Tmin were largely muted, one might be inclined to suggest that the primary forcing mechanism responsible for changes in Tmin are large scale processes including anthropogenic forcings and large-scale climate variability.

In contrast, Tmax trends from 1970–2006 as seen in the COOP network decidedly lack the homogenous warming seen in Tmin. During MAM and SON, the majority of stations with statistically significant trends warmed (85%), while during DJF and JJA the majority of stations with statistically significant trends cooled (~60%; see Figures 8c and 11). During DJF, although there were relatively few statistically significant stations (Figure 11a), about half the stations were negative in the sign of the trend and these negative trends were fairly evenly distributed throughout the state (not shown). However, during JJA (Figure 11b), the majority (15/23) stations that showed cooling were located in coastal regions.

The presence of cooling trends in Tmax from 1970–2006 during the two seasons, DJF and JJA, appear to have different physical mechanisms. The analysis of Lebassi et al. (2009) found widespread cooling trends in summertime (JJA) Tmax in the San Francisco Bay area and the Los Angeles area in the years since 1970. Their analysis suggested that daytime cooling in coastal basins was related to an enhanced sea-breeze circulation forced by additional warming in the interior. Our results also show cooling of Tmax along coastal regions during JJA (Figure 11b), although our results suggest this cooling was not ubiquitous for all coastal stations, with some coastal stations showing warming trends. The majority of significant Tmax cooling trends in DJF and JJA are constrained to 1970–2006 and don't appear in the longer time record (1918–2006). This suggests that either natural variability (e.g., Pacific decadal oscillation (PDO)) or a recent response to anthropogenic forcing may be at the root of recently observed summertime

coastal cooling. We note that although some of the stations from the COOP network may have data quality issues, the cooling results appear to be robust and suggest that local-scale changes may be obscured in coarser resolution observational datasets.

5.2 Analysis of COOP trends in DJF since 1970

An approach linking the covariability of temperature and precipitation is presented to provide insight into the overall neutral or weak warming trends found in Tmax trends over the state from 1970–2006. The overall lack of warming noted in DJF Tmax from across the state of California appears as an anomaly to the widespread warming observed across other seasons and for Tmin. A majority of stations across the state exhibited a significant negative correlation between DJF Tmax and DJF accumulated precipitation (Figure 12a). The correlation between precipitation and temperature trends was also discussed, although not extensively quantified by Cayan et al. (2008). The geographic representation of the temperature-precipitation covariability was strong ($r<-0.5$) across the Sierra Nevada, coast range, and interior portions of Southern California, suggesting that Tmax is suppressed during wet winters, and vice versa. In general, the synoptic-scale patterns that bring wintertime precipitation are associated with dynamical (cooler air mass) and thermodynamical (increased cloud cover, snow cover, and soil moisture) mechanisms that suppress Tmax. The only widespread regions void of the anticorrelation in temperature-precipitation records exist across the central and southern Central Valley. Extensive radiation fog often inundates the Central Valley during dry mid-winter blocking patterns, therein suppressing Tmax across the low-lying valley. By contrast, significant positive correlations between DJF Tmin and precipitation were observed for a majority of stations statewide from 1970–2006, suggesting that Tmin is suppressed during dry winters, and vice versa (Figure 12b). The strong covariability between Tmin and precipitation is argued to arise through

thermodynamic mechanisms (e.g., radiative cooling) associated with precipitation (e.g., cloud cover).

Over the 1970–2006 period, the state of California observed an increase in winter precipitation with 98% of stations showing positive, albeit, generally non-significant trends (10% of stations, most located in the northern portion of the state, showed statistically significant positive trends in precipitation). It is hypothesized that increases in precipitation over the last 35 years, and moreover the consortium of synoptic conditions associated with these increases, have acted to modulate regional trends for Tmax and Tmin. To account for the influence of precipitation on winter temperature trends across the state we remove the collinear influence of precipitation on temperature using Equation 1,

$$T_{i,R}(t) = T_i(t) - \alpha_i P_i'(t) \ , \qquad (1)$$

where $T_{i,R}(t)$ represents the residual temperature of a given station, i,; at time t, the regression coefficient of temperature to precipitation is α_i, and the seasonal precipitation anomaly is $P_i'(t)$. Winter Tmax and Tmin trends are calculated for both the observed time series and the residual time series so that the influence of trends in precipitation can be evaluated.

Observed trends in DJF Tmax for 1970–2006 were relatively weak across the state with a statewide trend of +0.07ºC dec^{-1} with only a few stations showing a significant positive trend. Linear trends of the residual temperature, after removing the linear contribution from winter precipitation, exhibited over twice as many stations (12%) with statistically significant warming, and a statewide trend of +0.12ºC dec^{-1}. By contrast, observed trends in DJF Tmin for COOP stations for 1970–2006 exhibited a statewide trend of +0.35ºC dec^{-1} with over a third of all stations showing significant warming trends. Upon removal of the collinear influence of precipitation, the statewide trend was +0.22ºC dec^{-1}. It is presently unclear whether the increases in DJF precipitation observed during this period are consistent with anthropogenic climate

change or natural variability; however, it is clear that the lack of widespread warming in Tmax, and high rate of warming in Tmin can be partially accounted for by increases in precipitation.

6. Discussion of forcing mechanisms

This analysis offers two important diagnostics that may be useful in characterizing statewide changes in temperature during 1918–2006. One is the striking consistency in widespread shifts of temperature that appear throughout the state, and the other is the notable difference between Tmin and Tmax temperature variations. For example, the remarkably consistent end of cool Tmin periods in 1958 and the similarly common beginning of warm periods around 1978 suggest a universal change in California-wide climate patterns on Tmin that are not uniformly reflected in Tmax. The disparity between temperature signals from Tmin and Tmax suggests distinctly separate forcing mechanisms that operate at different spatial scales. Alfaro et al. (2006) showed that summertime variations in Tmin over the central and western U.S. are controlled more by larger-scale forcings (e.g., sea surface temperatures), while Tmax is controlled more by local-scale forcings (e.g., soil moisture and cloudiness).

The patterns of temperature change for Tmin and Tmax provide clues about the role of different forcing mechanisms on California's climate. Both natural and anthropogenic forcing mechanisms have been shown to influence global and regional climate (e.g., IPCC 2007). Climate attribution studies have examined the influence of anthropogenic forcing (e.g., Bonfils et al. 2008) and internal climate variability (e.g., Hoerling et al. 2010) on regional climate. Although it is increasingly difficult to attribute changes at local scales due to weak signal-to-noise ratios (e.g., Hegerl et al. 2007), several forcing mechanisms are hypothesized to have influenced temperatures in California. Increased concentrations of GHGs are hypothesized to directly (i.e., via radiative forcing) increase Tmax and Tmin at similar rates over large spatial scales (i.e., Zhou et al. 2009). Increased anthropogenic aerosols are hypothesized to decrease

Tmax and have a stronger regional signal that may vary over time. Indirect mechanisms associated with these anthropogenic-forcing mechanisms may result in more complex regional signatures. For example, changes in clouds, as a consequence of modified aerosol concentration, atmospheric water vapor, soil moisture, or changes in ocean-atmosphere circulation would also be expected to differentially influence Tmax and Tmin. California's land surface has also changed profoundly over the last century, with urbanization and large-scale irrigation among the largest changes observed. Urbanization appears to raise primarily Tmin (e.g., LaDochy et al. 2007), while irrigation appears to both cool maximum temperatures and warm minimum temperatures (e.g., Bonfils and Lobell 2007, Kueppers et al. 2007). Finally, superimposed on these external forcings is natural internal variability manifested through large-scale coupled atmosphere-ocean phenomena, such as El Nino-Southern Oscillation and the PDO, that have a noted influence on temperature and precipitation across California (e.g., Redmond and Koch, 1991; LaDochy et al. 2007). Changes in atmospheric circulation regimes over the latter half of the 20th century have been shown to influence regional temperatures (e.g., Wu and Straus, 2004; Abatzoglou and Redmond, 2007; Abatzoglou, 2010) and are hypothesized to have influenced the observed evolution of Tmax and Tmin across California.

In the above MWZ analysis, the patterns of annual temperature change for Tmin (Figure 6b) indicate steady widespread warming (cool periods to warm periods) over the 80-year period, suggesting large-scale forcing such as increases in GHGs. This pattern is similar for different seasons except MAM (not shown), where a statewide cool period is found between the 1940s and 1970s. While this corresponds to the well-documented cold period of the PDO (Mantua et al. 1997), it is presently unclear why spring minimum temperatures would be affected more than other seasons if the PDO is responsible for these changes.

For Tmax, the patterns identified by the MWZ method (Figure 6a) vary more in space and time compared to Tmin. The most pronounced pattern in the annual variations is warm-cold-warm, where a warm period early in the century is followed by a cool period mid century and then another warm period towards the end of the record. While the MWZ analysis for each season (not shown) generally follows this pattern, there are some distinct variations. For example, during MAM a very consistent statewide cooling period (in 80% of the stations) was found between the late 1940s and the mid 1960s. Because this pattern is so consistent throughout the state, it is suggested that variability associated with large-scale circulation is responsible, rather than a more localized signature associated with land-use change or aerosols. However, during JJA, over 70% of the stations from irrigated areas (i.e., North Central Region, Sacramento-Delta Region, and San Joaquin Valley Region) showed cooling periods between 1920 and 1980, and warming since 1990 or 2000. In this case, one would suspect that irrigation, which grew in California from the early century to around the 1980s, is a likely contributor to these changes. While this analysis cannot directly attribute any of these forcings to observed evolution of regional temperature trends, we present this analysis to provide guidance for later climate attribution studies.

7. Summary and conclusions

California temperatures have seen significant changes over the last 80 years, with variations both in time and in space and differential changes in Tmin and Tmax. In general, the southern part of the state, and the southern deserts in particular, has experienced the greatest amount of warming, and this warming has accelerated over the last 35 years. The greater warming in Southern California compared to Northern California and the recent amplification in warming has been more pronounced in Tmax compared to Tmin. Although Tmin also show significant warming, this warming is more uniformly distributed throughout the state. Since

1970, the largest warming is found during MAM, both for Tmin and Tmax. The similar rates of warming for Tmin and Tmax in Southern California are distinct from the larger Tmin warming in Northern California. In general, DJF shows the weakest warming for both Tmin and Tmax throughout the state.

Mann-Whitney Z analyses conducted on annual USHCN station data identify broad-scale consecutive warm and cold years throughout the 88-year record and distinct patterns for Tmin and Tmax. For Tmin, colder years are prevalent between 1920 and 1958, while warmer years are observed after 1978. The pattern in Tmax is quite different, with warmer years found between 1925 and 1942 and again starting in the period 1985 to 1995, while cooler years are observed between 1945 and 1975. The remarkable statewide shift in warming and cooling years for Tmin suggests large-scale forcing, a distinctly different pattern from the warming and cooling seen in Tmax, which suggests more local-scale forcing. The MWZ method is shown to be a better analysis tool for analyzing multi-decadal variability compared to linear trends.

Further differences between Tmin and Tmax are found by examining seasonal trends in the individual COOP data since 1970. Although large-scale warming is found for Tmin trends during all seasons, during DJF and JJA we find that about half the significant Tmax trends are cooling. During DJF, the lack of warming for Tmax throughout California is found only since 1970, and it is suggested that an increase in precipitation (and thus cloudiness) over California in the last 35 years has masked warming. By contrast, increases in winter precipitation since 1970 are also shown to have accelerated the rate of warming of Tmin, therein providing insight into contrasting mechanisms behind regional Tmax and Tmin trends. Patterns of cooling during JJA are largely constrained to coastal areas, which suggest a relationship with ocean temperatures.

A variety of forcing mechanisms appear to have influenced climate in California over different space and time scales. Foremost are the increases in well-mixed greenhouse gases that

have been carefully documented and attributed to most of the global- and continental-scale warming observed since 1970. However, other changes such as land-use changes, variations in precipitation, regional-to-local feedback processes, and changes in ocean temperatures and sea breeze are also likely to have played a role in the spatial and temporal character of California temperatures over the past century. The aim of our study has been to characterize the changes in California's climate so that future attribution studies can be performed to better understand the interrelationships between the various forcing mechanisms. We suggest that the Mann-Whitney Z analysis, coupled with output from downscaled and regional climate models, would be an excellent tool for such attribution studies, especially where identifying the role of local- versus large-scale forcing is important. This work has already begun with the ultimate aim of improving our projections of future changes in California's climate.

Acknowledgements We thank Bereket Lebassi for help in acquiring the NWS COOP dataset and Professor Bob Bornstein for many helpful discussions. This work was supported by NSF's Faculty Early Career Development (CAREER) Program, Grant ATM-0449996.

Table 1. Annual and seasonal maximum and minimum temperatures trends (°C dec^{-1}) during 1918-2006 for California and the 11 defined climate regions based on the USHCN network. The * symbol next to the value indicates that trends are statistically significant at the 95% confidence level and the number adjacent to each region indicates the number of stations in that region.

SEASON	MAXIMUM	MINIMUM	SEASON	MAXIMUM	MINIMUM
California (58)			***E. Sacramento-Delta Region (7)***		
Annual	0.071*	0.17*	Annual	0.17*	0.26*
DJF	0.078	0.14*	DJF	0.14*	0.19*
MAM	0.088	0.15*	MAM	0.21*	0.23*
JJA	0.069	0.21*	JJA	0.16*	0.32*
SON	0.045	0.18*	SON	0.17*	0.29*
Northern California (33)			***F. Central Coast Region (3)***		
Annual	0.05	0.17*	Annual	0.12*	0.15*
DJF	0.058	0.12*	DJF	0.12*	0.12*
MAM	0.067	0.15*	MAM	0.17*	0.17*
JJA	0.053	0.22*	JJA	0.13*	0.20*
SON	0.024	0.17*	SON	0.059	0.10*
Southern California (25)			***G. San Joaquin Valley Region (7)***		
Annual	0.10*	0.17*	Annual	0.016	0.17*
DJF	0.1	0.17*	DJF	-0.016	0.12*
MAM	0.11*	0.16*	MAM	0.065	0.14*
JJA	0.11*	0.17*	JJA	-0.003	0.21*
SON	0.078*	0.18*	SON	0.008	0.21*
A. North Coast Region (3)			***H. South Coast Region (5)***		
Annual	0.085*	0.12*	Annual	0.13*	0.18*
DJF	0.096*	0.13*	DJF	0.16*	0.22*
MAM	0.098*	0.15*	MAM	0.12*	0.14*
JJA	0.11*	0.13*	JJA	0.15*	0.19*
SON	0.028	0.053	SON	0.074*	0.18*
B. North Central Region (12)			***I. South Interior Region (3)***		
Annual	0.026	0.17*	Annual	0.16*	0.22*
DJF	0.045	0.12*	DJF	0.26*	0.19*
MAM	0.002	0.12*	MAM	0.21*	0.20*
JJA	0.009	0.20*	JJA	0.057	0.21*
SON	0.039	0.17*	SON	0.092	0.27*
C. Northeast Region (3)			***J. Mojave Desert Region (4)***		
Annual	-0.044	0.20*	Annual	0.13*	0.093*
DJF	0.091	0.12	DJF	0.13*	0.13*
MAM	-0.004	0.18*	MAM	0.16*	0.12*
JJA	-0.081	0.30*	JJA	0.095	0.085
SON	-0.19*	0.19*	SON	0.12*	0.012
D. Sierra Region (5)			***K. Sonoran Desert Region (6)***		
Annual	-0.036	0.058*	Annual	0.10*	0.17*
DJF	-0.074	0.002	DJF	0.05	0.18*
MAM	0.01	0.077	MAM	0.066	0.17*
JJA	0.062	0.13*	JJA	0.18*	0.13*
SON	-0.097	0.023	SON	0.11*	0.22*

Table 2. As in Table 1 except the trends are computed between 1970-2006.

SEASON	MAXIMUM	MINIMUM	SEASON	MAXIMUM	MINIMUM
California (58)			***E. Sacramento-Delta Region (7)***		
Annual	0.27*	0.31*	Annual	0.34*	0.37*
DJF	0.13	0.28	DJF	0.25	0.33
MAM	0.33	0.40*	MAM	0.34	0.41*
JJA	0.26	0.32*	JJA	0.32*	0.38*
SON	0.34	0.24	SON	0.40*	0.34*
Northern California (33)			***F. Central Coast Region (3)***		
Annual	0.21*	0.29*	Annual	0.15	0.19
DJF	0.098	0.26	DJF	0.12	0.1
MAM	0.24	0.35*	MAM	0.31	0.3
JJA	0.18	0.32*	JJA	-0.032	0.24*
SON	0.32	0.2	SON	0.16	0.1
Southern California (25)			***G. San Joaquin Valley Region (7)***		
Annual	0.35*	0.37*	Annual	0.30*	0.26*
DJF	0.18	0.31	DJF	0.17	0.22
MAM	0.46*	0.49*	MAM	0.33	0.3
JJA	0.36*	0.33*	JJA	0.37*	0.25*
SON	0.35*	0.33*	SON	0.3	0.25
A. North Coast Region (3)			***H. South Coast Region (5)***		
Annual	0.14	0.20*	Annual	0.17	0.41*
DJF	0.16	0.2	DJF	0.16	0.44*
MAM	0.19	0.3	MAM	0.19	0.56*
JJA	0.22	0.28*	JJA	0.19	0.36*
SON	-0.058	0.005	SON	0.14	0.29*
B. North Central Region (12)			***I. South Interior Region (3)***		
Annual	0.26*	0.29*	Annual	0.42*	0.26*
DJF	0.11	0.31	DJF	0.17	0.2
MAM	0.22	0.33*	MAM	0.58*	0.42*
JJA	0.24	0.27*	JJA	0.45*	0.22
SON	0.43	0.21	SON	0.46*	0.21
C. Northeast Region (3)			***J. Mojave Desert Region (4)***		
Annual	0.22	0.38*	Annual	0.49*	0.39*
DJF	0.043	0.38	DJF	0.27	0.36*
MAM	0.34	0.43*	MAM	0.67*	0.52*
JJA	0.13	0.41*	JJA	0.43*	0.32*
SON	0.35	0.27	SON	0.56*	0.37*
D. Sierra Region (5)			***K. Sonoran Desert Region (6)***		
Annual	0.08	0.21*	Annual	0.36*	0.51*
DJF	-0.12	0.06	DJF	0.13	0.37*
MAM	0.14	0.35*	MAM	0.57*	0.68*
JJA	0.051	0.38*	JJA	0.35*	0.47*
SON	0.25	0.018	SON	0.37	0.54*

Figure Captions

Figure 1. Map of the USHCN stations used in this study, where each station name is indicated on the left.

Figure 2. Map of the COOP stations used in this study.

Figure 3. California annual maximum (top) and minimum (bottom) temperatures computed from the USHCN network between 1918-2006. The linear trends (in ºC dec^{-1}) are shown where an asterisk (*) indicates that the trend is statistically significant at the 95% confidence level. Accompanying each statewide time series, statistically significant Z values (at the 95% and 99% confidence level) for the MWU analysis are shown, where blue shading indicates cool periods and red shading indicates warm periods.

Figure 4. Annual temperature trends (ºC dec^{-1}) for the 11 climate regions labeled A-K computed between 1918-2006 for Tmax (left) and Tmin (right). Adjacent to each region label is the annual trend for Tmax and Tmin, where the trends that are statistically significant at the 95% confidence level are indicated with an asterisk (*).

Figure 5. A comparison of the statewide and regional annual (a) Tmax and (b) Tmin trends (ºC dec^{-1}) for two time periods, 1918-2006 and 1970-2006, where the bars are solid when the computed trend is statistically significant (95% confidence level) and hashed when the trend is not statistically significant.

Figure 6. Z values computed using running Mann-Whitney U statistics for annual temperatures during 1918-2006 for (a) Tmax and (b) Tmin from the USHCN stations. Red colors denote warming temperatures while blue colors denote cooling temperatures, with the shading from darkest to lightest indicating statistical significance at the 99%, 95% and 90% confidence level respectively. Each of the individual station names is given on the right, while the corresponding regions are indicated on the left.

Figure 7. Map showing statistically significant (95% confidence level) warming and cooling trends (ºC dec^{-1}) between 1918-2006 for annual (a) Tmax and (b) Tmin temperatures collected at USHCN stations throughout California. Red circles denote warming trends and blue circles denote cooling trends, while the number of statistically significant warming and cooling stations is given at the bottom.

Figure 8. The percentage of statistically significant (95% confidence level) warming and cooling trends for annual and seasonal Tmax and Tmin during the periods of 1918-2006 for the a) USHCN data, b) 1970-2006 for the USHCN data, and c) 1970-2006 for the COOP data.

Figure 9. Map showing statistically significant (95% confidence level) warming and cooling trends (ºC dec^{-1}) between 1970-2006 for annual (a) Tmax and (b) Tmin temperatures collected at USHCN stations throughout California. Red circles denote warming trends and blue circles denote cooling trends, while the number of statistically significant warming and cooling stations is given at the bottom.

Figure 10. As in Figure 9 except that the trends are computed from the COOP network.

Figure 11. As in Figure 9 except that the trends are computed from the COOP network and only for Tmax during (a) DJF and (b) JJA.

Figure 12. Statistically significant correlation coefficients for accumulated precipitation and (a) winter (DJF) maximum temperature and (b) winter DJF minimum temperature over the period 1970-2006 for COOP stations within California.

References

Abatzoglou JT (2010) Influence of the PNA on declining mountain snowpack in the Western United States. Int J Climatol, doi:10.1002/joc.2137

Abatzoglou JT, Redmond KT, Edwards LE (2009) Classification of regional climate variability in the State of California. Appl Meteorol and Climatol 48:1527-1541

Abatzoglou JT, Redmond KT (2007) The asymmetry of trends in spring and autumn temperature and circulation regimes over western North America. Geophys Res Lett 34, doi:10.1029/2007GL030891

Alfaro EJ, Gershunov A, Cayan D (2006) Prediction of summer maximum and minimum temperature over the Central and Western United States: The roles of soil moisture and sea surface temperature. J Clim 19:1407-1421

Bonan GB (2001) Observational evidence for reduction of daily maximum temperature by croplands in the midwest United States. J Clim 14:2430-2442

Bonfils C, Duffy PB, Santer BD, Wigley TML, Lobell DB, Phillips TJ, Doutriaux C (2008) Identification of external influences on temperatures in California. Clim Change 87 suppl 1: S43-S55, doi:10.1007/s10584-007-9374-9

Bonfils C, Lobell DB (2007) Empirical evidence for a recent slowdown in irrigation-induced cooling. Proc Natl Acad Sci 104:13582-13587

Bonfils C, Duffy PB, Lobell DB (2006) Comments on "methodology and results of calculating central California surface temperature trends: evidence of human-induced climate change? J Clim 20:4486-4489

Cayan DR, Maurer EP, Dettinger MD, Tyree M, Hayhoe K (2008) Climate change scenarios for the California region. Clim Change 87 suppl 1: S21-S42, doi:10.1007/s10584-007-9377-6

Christy JR, Norris WB, Redmond KT, Gallo KP (2006) Methodology and results of calculating central California surface temperature trends: Evidence of human-induced climate change? J Clim 19:548-563

Cordero E, Forster PMdF (2006) Stratospheric variability and trends in models used for the IPCC AR4. Atmos Chem Phys 6:5369-5380

Hayhoe K, Cayan D, Field CB, Frumhoff PC, Maurer EP, Miller NL, Moser SC, Schneider SH, Cahill KN, Cleland EE, Dale L, Drapek R, Hanemann RM, Kalkstein LS, Lenihan J, Lunch CK, Neilson RP, Sheridan SC, Verville JH (2004) Emissions pathways, climate change, and impacts on California. Proc Natl Acad Sci 101:12422-12427

Hegerl GC, Zwiers FW, Braconnot P, Gillett NP, Luo Y, Marengo J, Nicholls N, Penner JE, Stott PA (2007) Understanding and attributing climate change. Chapter 9 in Climate change 2007: the physical science basis. Contribution of Working Group 1 to the Fourth Assessment Report on the Intergovernmental Panel on Climate Change. Cambridge University Press, Cambridge: 663-745

Hoerling M, Eischeid J, Perlwitz J (2010) Regional precipitation trends: Distinguishing natural variability from anthropogenic forcing. J Clim 23:2131-2145

IPCC (2007) Climate change 2007: the physical science basis. Contribution of Working Group 1 to the Fourth Assessment Report on the Intergovernmental Panel on Climate Change. Cambridge University Press, Cambridge

Kalnay E, Cai M (2003) Impact of urbanization and land-use change on climate. Nature 423:528-531

Kueppers LM, Snyder MA, Sloan LC (2007) Irrigation cooling effect: Regional climate forcing by land-use change. Geophys Res Lett 34: L03703, doi:10 1029/2006GL028679

LaDochy S, Medina R, Patzert W (2007) Recent California climate variability: spatial and temporal patterns in temperature trends. Clim Res 33:159-169
Lebassi B, Gonzalez J, Fabris D, Maurer E, Miller N, Milesi C, Switzer P, Bornstein R (2009) Observed 1970-2005 cooling of summer daytime temperatures in coastal California. J Clim: in press
Lund R, Seymour L, Kafadar K (2001) Temperature trends in the United States. Environmetrics 12:673-690, doi:610.1002/env.1468
Mantua NJ, Hare SR, Zhang Y, Wallace JM, Francis RC (1997) A Pacific interdecadal climate oscillation with impacts on salmon production. Bull Amer Meteor Soc 78:1069-1079
Mauget SA (2003a) Intra- to multi-decadal climate variability over the Continental United States: 1932-1999. J Clim 16:2215-2231
Mauget SA (2003b) Multi-decadal regime shifts in U.S. streamflow, precipitation, and temperature at the end of the Twentieth Century. J Clim 16:3905-3916
Mendenhall W, Wackerly DD, Sheaffer RL (1990) Mathematical Statistics with Applications. PWS-Kent, Boston
Peterson TC (2003) Assessment of urban versus rural in situ surface temperature in the contiguous United States: no difference found. J Clim 16:2941-2959
Redmond KT, Koch RW (1991) Surface climate streamflow variability in the western United States and their relationship to large-scale circulation indices. Water Resources Res 27:2381-2399, doi:10.1029/91WR00690
Santer BD, Wigley TML, Boyle JS, Gaffen DJ, Hnilo JJ, Nychka D, Parker DE, Taylor KE (2000) Statistical significance of trends and trend differences in layer-average atmospheric temperature time series. J Geophys Res Atmos 105(D6):7337-7356
Saxena VK, Yu S (1998) Searching for a regional fingerprint of aerosol radiative forcing in the southeastern US. Geophys Res Lett 25:2833-2836
Stafford JM, Wendler G, Curtis J (2000) Temperature and precipitation of Alaska: 50 year trend analysis. Theor Appl Climatol 67:33-44
Vose RS, Easterling DR, Gleason B (2005) Maximum and minimum temperature trend for the globe: An update through 2004. Geophys Res Lett 32:L23822, doi:23810.21029/22005GL024379
Wild M, Ohmura A, Makowski K (2007) Impact of global dimming and brightening on global warming. Geophys Res Lett 34, doi:10.1029/2006GL028031
Wilks DS (1995) Statistical Methods in the Atmospheric Sciences. Academic Press, San Diego
Williams CN, Menne MJ, Vose R, Eastering DR (2007) United States Historical Climatology Network monthly temperature and precipitation data. Oak Ridge National Laboratory, Oak Ridge, Tennessee: ORNL/CDIAC-187
Wu QG, Straus DM (2004) On the existence of hemisphere-wide climate variations. J Geophys Res Atmos 109, D06118, doi: 10.1029/2003JD004230
Yang F, Kumar A, Wang W, Juang H-MH, Kanamitsu M (2001) Snow-albedo feedback and seasonal climate variability over North America. J Clim 14:4245-4248
Zhou LM, Dickinson RE, Dirmeyer P, Dai A, Min S-K (2009) Spatiotemporal patterns of changes in maximum and minimum temperatures in multi-model simulations. Geophys Res Lett 36, L02702, doi:10.1029/2008GL036141

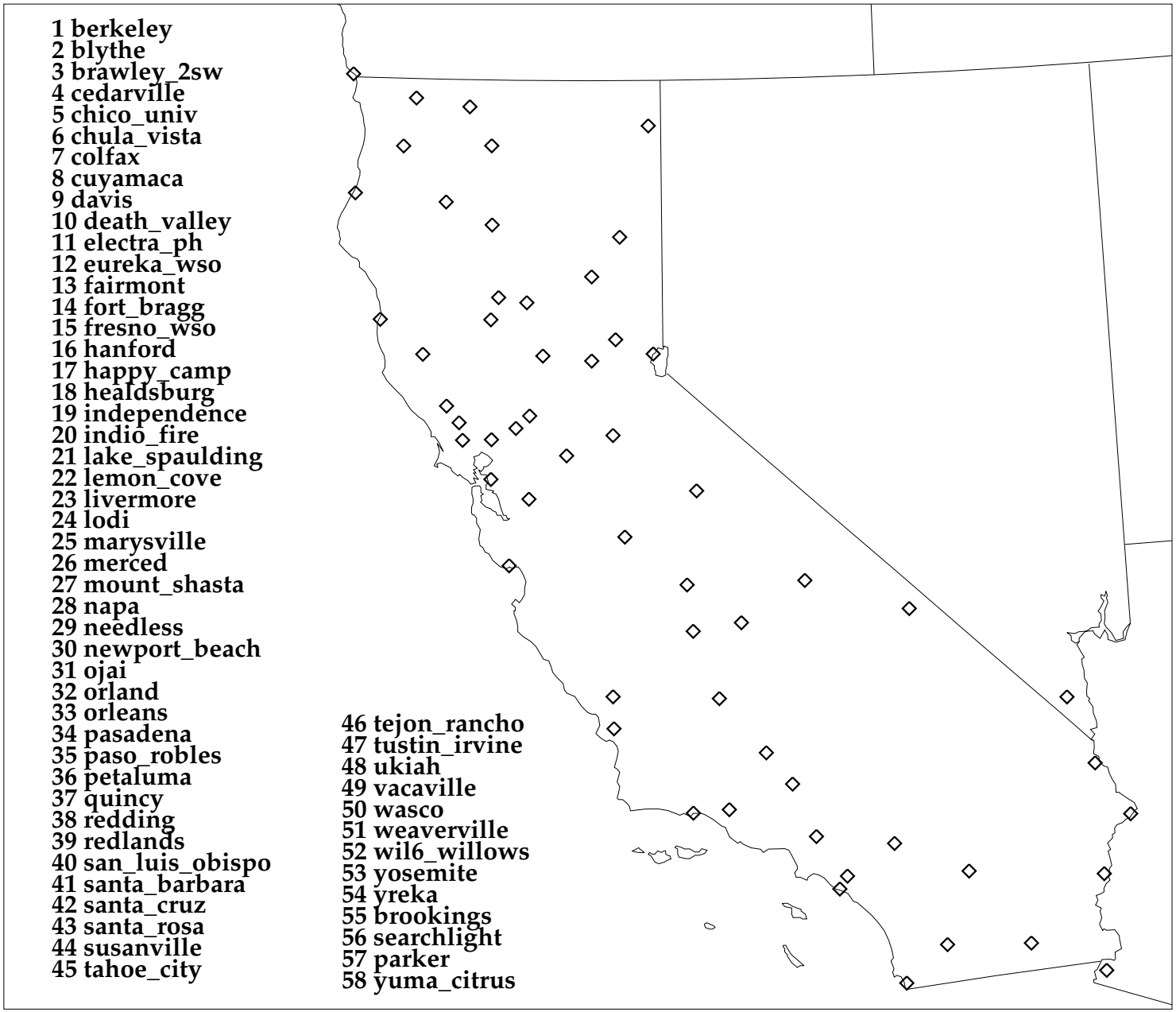
1 berkeley
2 blythe
3 brawley_2sw
4 cedarville
5 chico_univ
6 chula_vista
7 colfax
8 cuyamaca
9 davis
10 death_valley
11 electra_ph
12 eureka_wso
13 fairmont
14 fort_bragg
15 fresno_wso
16 hanford
17 happy_camp
18 healdsburg
19 independence
20 indio_fire
21 lake_spaulding
22 lemon_cove
23 livermore
24 lodi
25 marysville
26 merced
27 mount_shasta
28 napa
29 needless
30 newport_beach
31 ojai
32 orland
33 orleans
34 pasadena
35 paso_robles
36 petaluma
37 quincy
38 redding
39 redlands
40 san_luis_obispo
41 santa_barbara
42 santa_cruz
43 santa_rosa
44 susanville
45 tahoe_city
46 tejon_rancho
47 tustin_irvine
48 ukiah
49 vacaville
50 wasco
51 weaverville
52 wil6_willows
53 yosemite
54 yreka
55 brookings
56 searchlight
57 parker
58 yuma_citrus

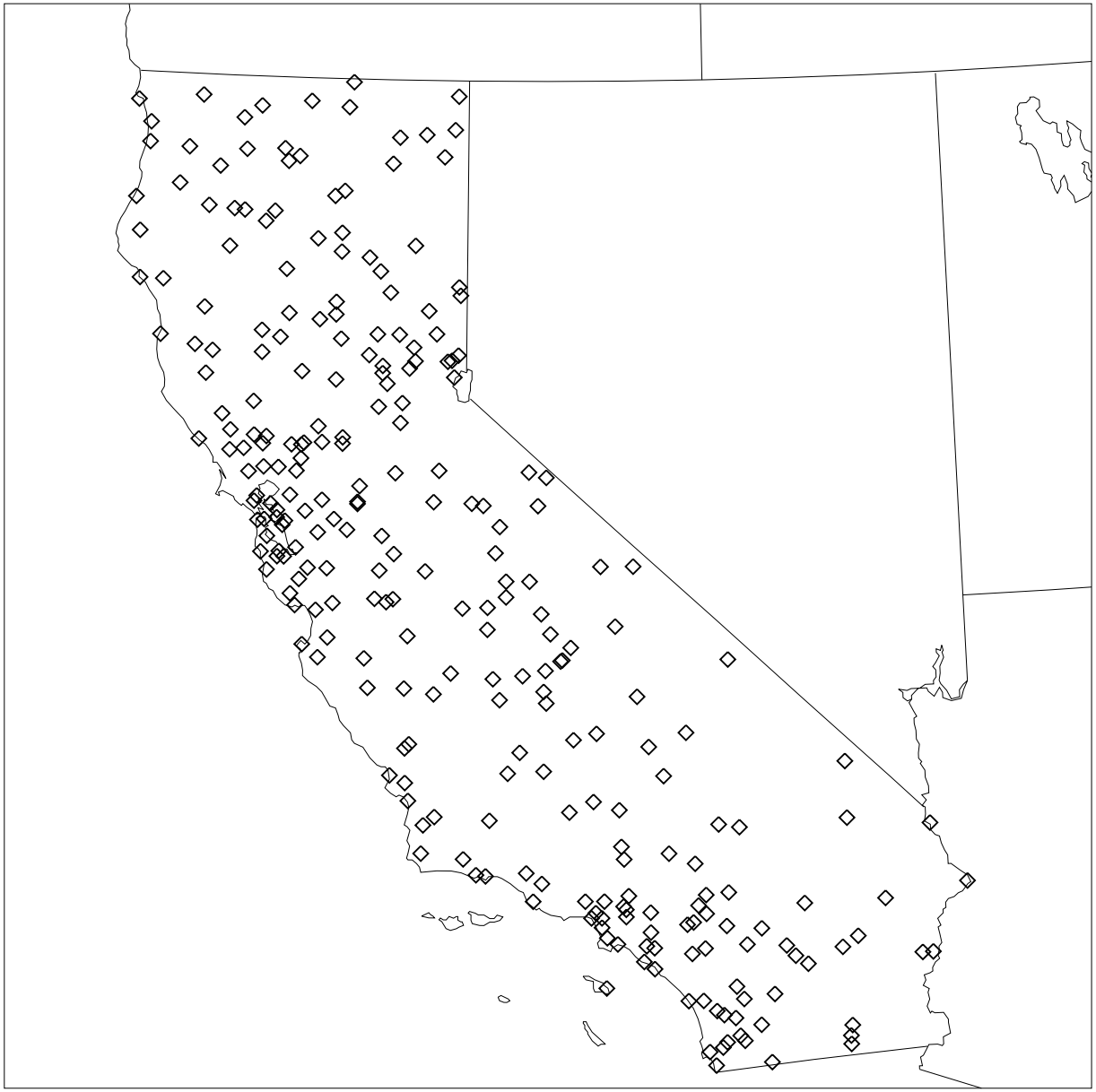

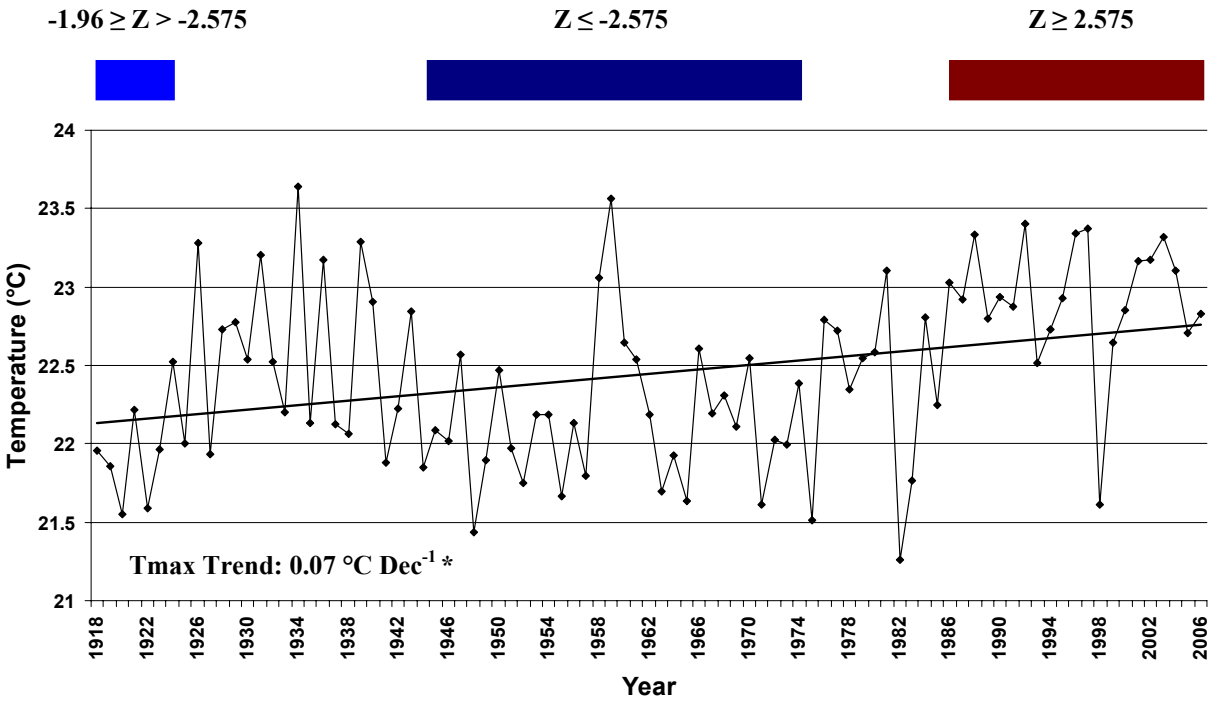
-1.96 ≥ Z > -2.575
Z ≤ -2.575
Z ≥ 2.575
Temperature (°C)
Tmax Trend: 0.07 °C Dec-1 *
Year

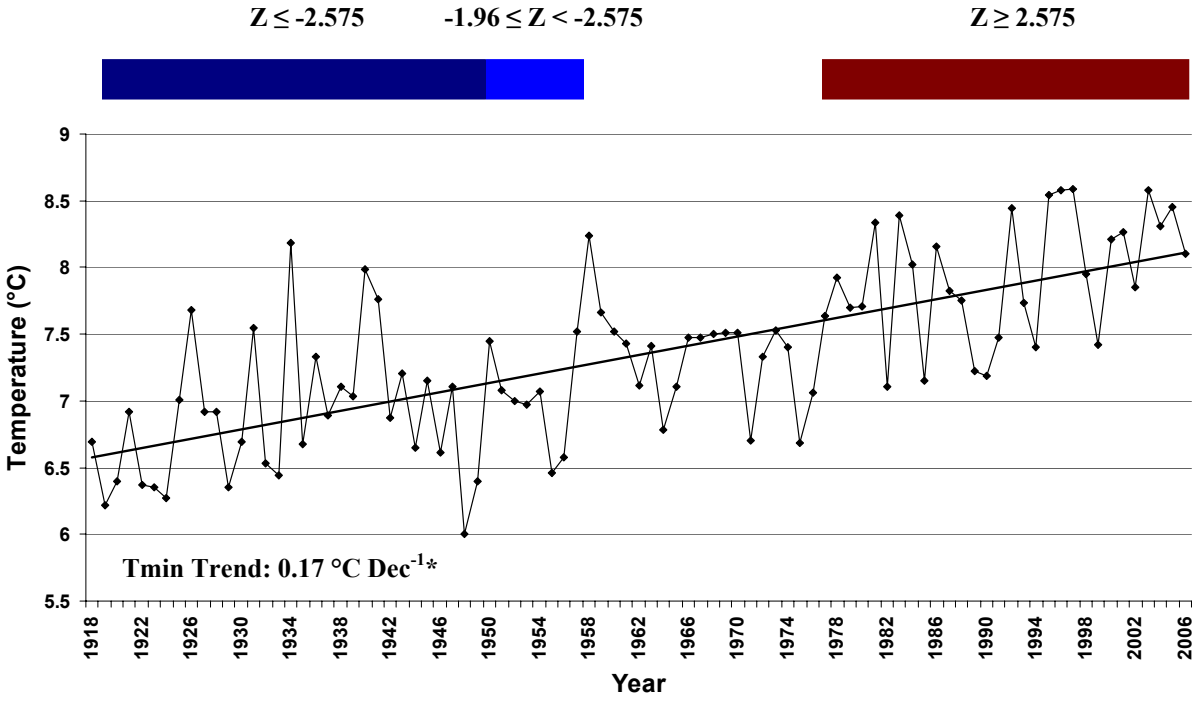
Z ≤ -2.575
-1.96 ≤ Z < -2.575
Z ≥ 2.575
Temperature (°C)
Tmin Trend: 0.17 °C Dec-1*
Year

Figure 3

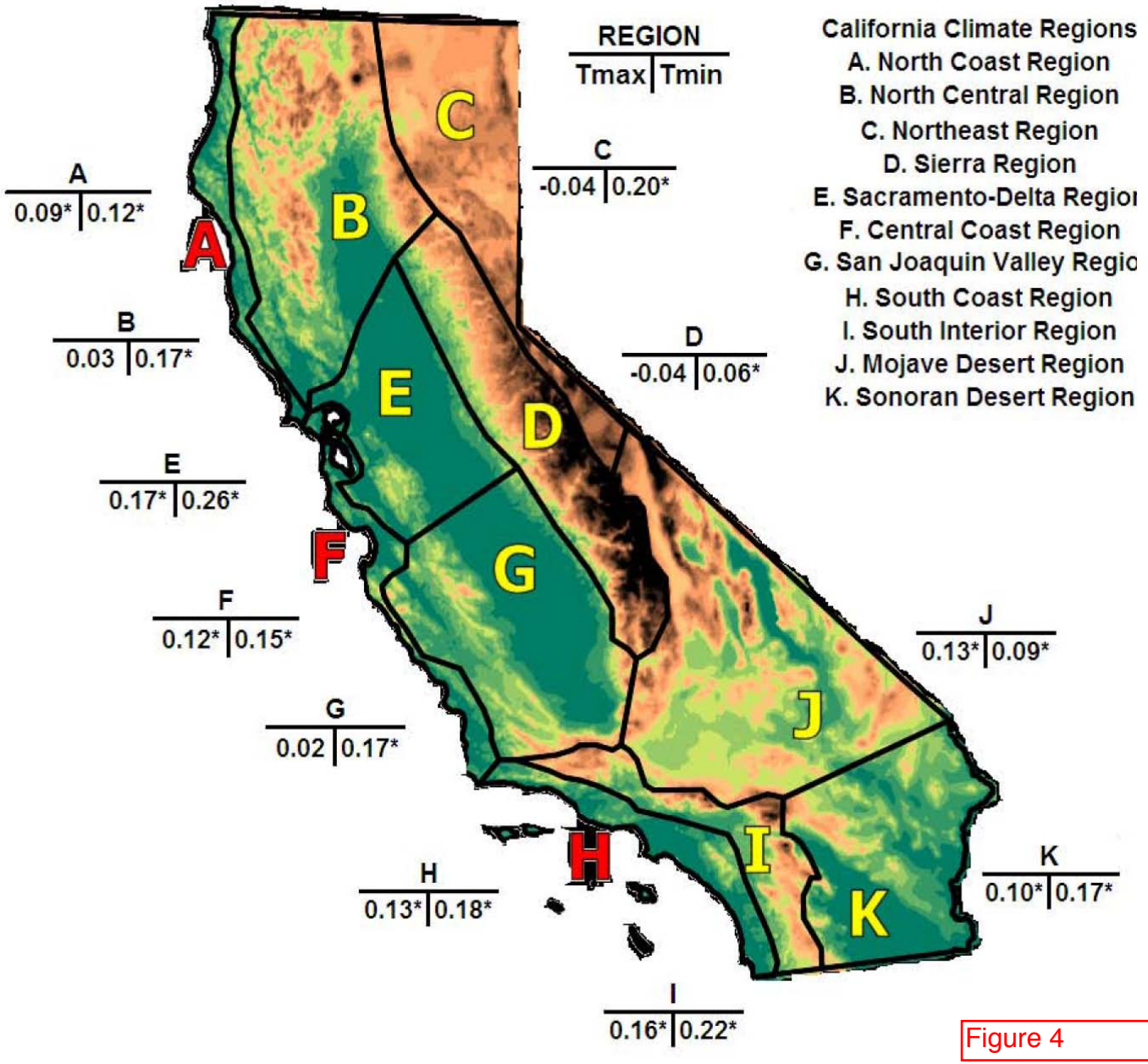
REGION
Tmax | Tmin
California Climate Regions
A. North Coast Region
B. North Central Region
C. Northeast Region
D. Sierra Region
E. Sacramento-Delta Regio
F. Central Coast Region
G. San Joaquin Valley Regio
H. South Coast Region
I. South Interior Region
J. Mojave Desert Region
K. Sonoran Desert Region
A
0.09* | 0.12*
B
0.03 | 0.17*
C
-0.04 | 0.20*
D
-0.04 | 0.06*
E
0.17* | 0.26*
F
0.12* | 0.15*
G
0.02 | 0.17*
H
0.13* | 0.18*
I
0.16* | 0.22*
J
0.13* | 0.09*
K
0.10* | 0.17*

Figure 4

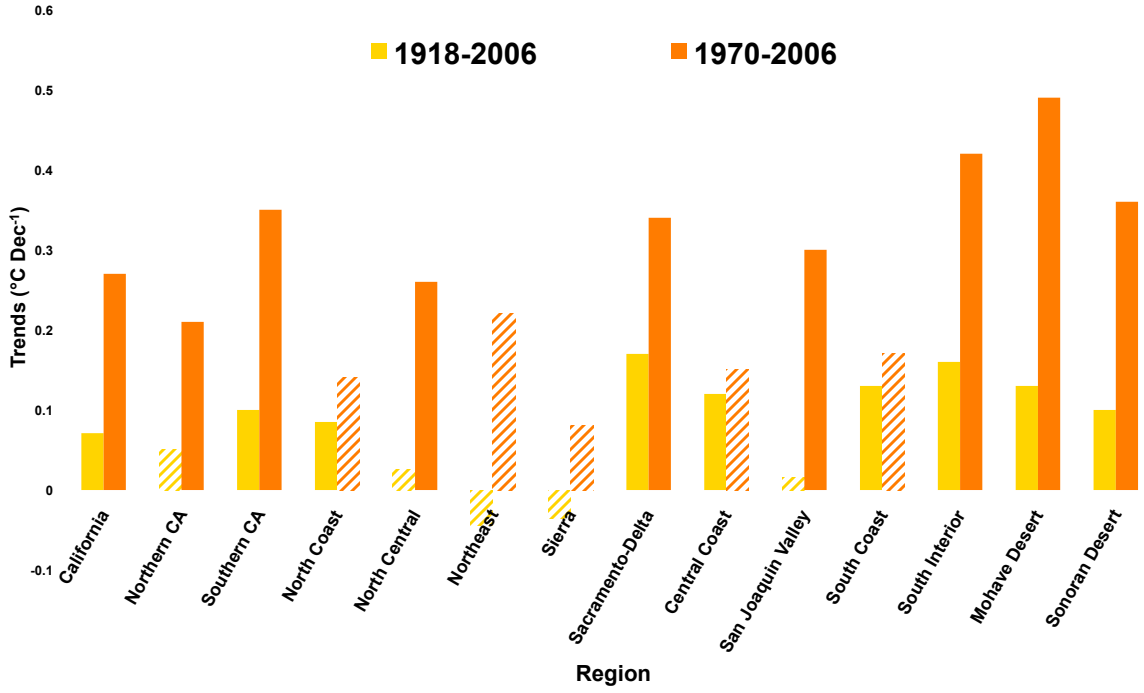
1918-2006
1970-2006
Trends (°C Dec-1)
0.6
0.5
0.4
0.3
0.2
0.1
0
-0.1
California
Northern CA
Southern CA
North Coast
North Central
Northeast
Sierra
Sacramento-Delta
Central Coast
San Joaquin Valley
South Coast
South Interior
Mohave Desert
Sonoran Desert
Region

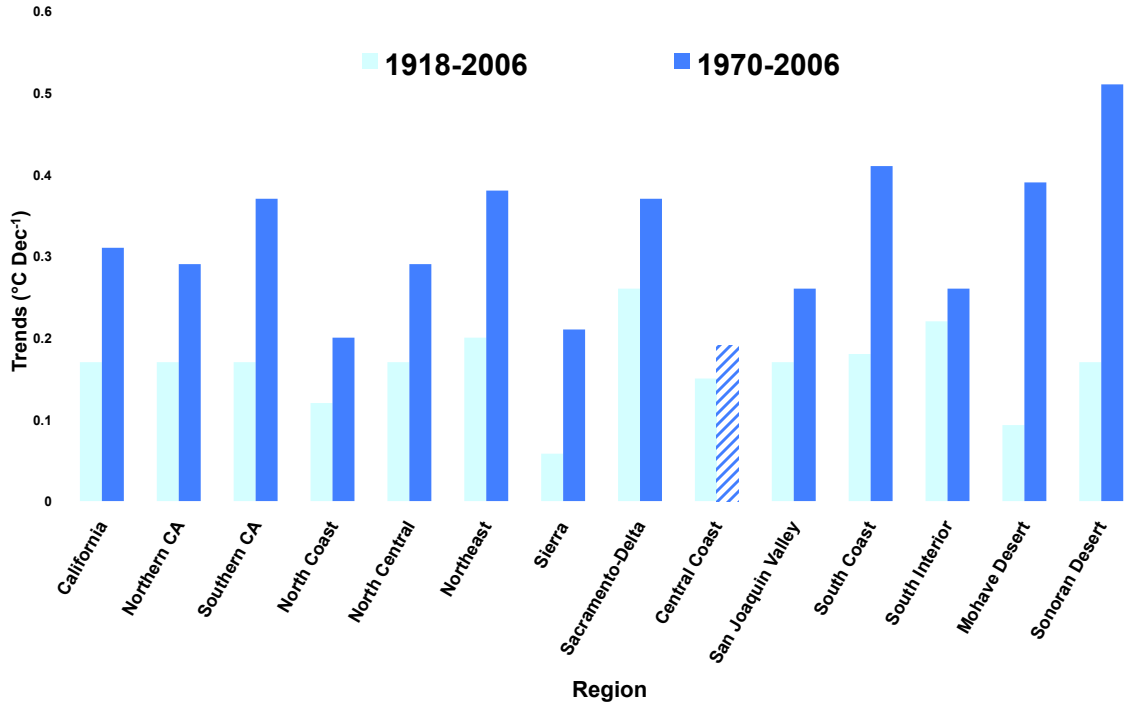
1918-2006
1970-2006
Trends (°C Dec-1)
0.6
0.5
0.4
0.3
0.2
0.1
0
California
Northern CA
Southern CA
North Coast
North Central
Northeast
Sierra
Sacramento-Delta
Central Coast
San Joaquin Valley
South Coast
South Interior
Mohave Desert
Sonoran Desert
Region

Figure 5

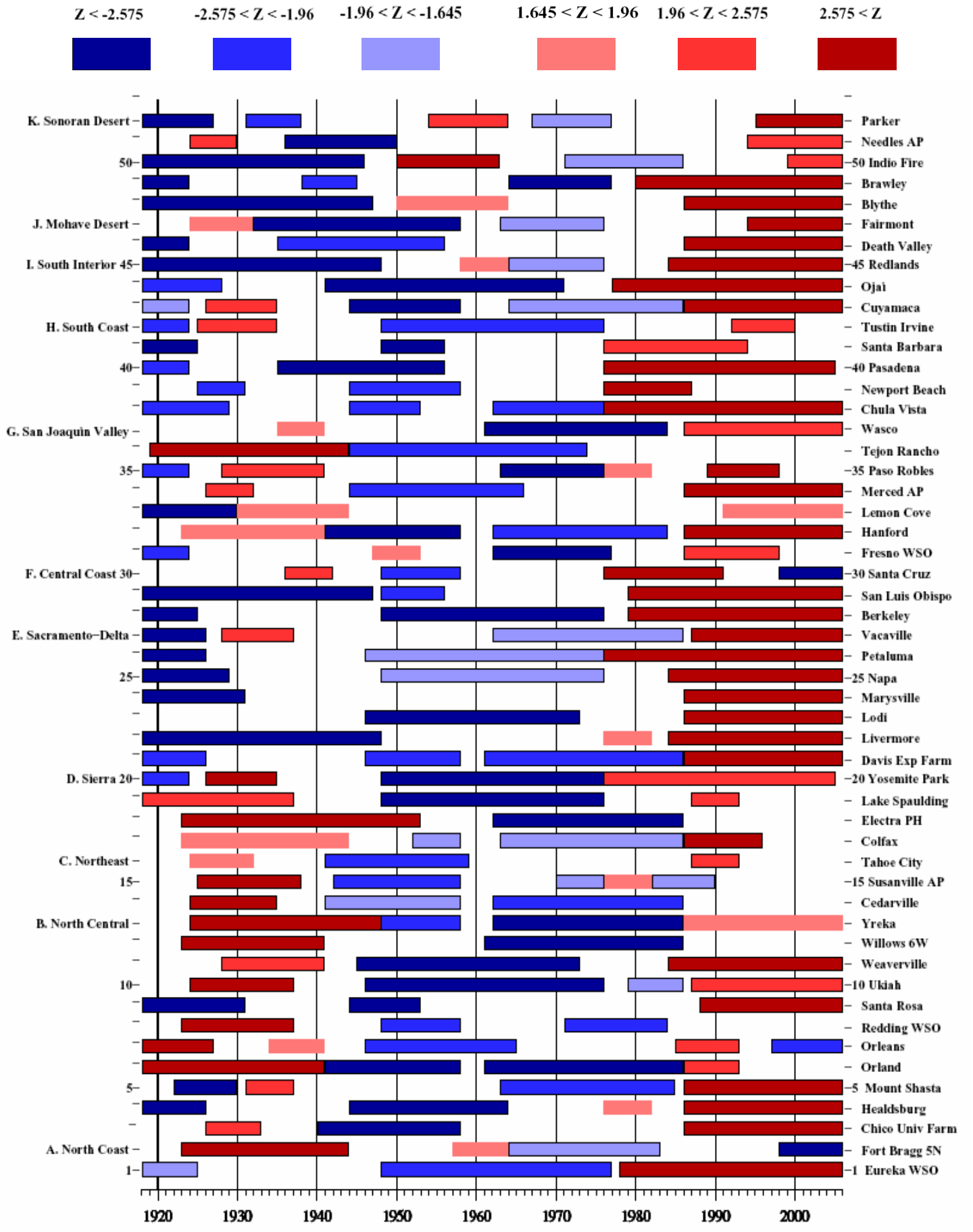
Z < -2.575
-2.575 < Z < -1.96
-1.96 < Z < -1.645
1.645 < Z < 1.96
1.96 < Z < 2.575
2.575 < Z
K. Sonoran Desert
J. Mohave Desert
I. South Interior
H. South Coast
G. San Joaquin Valley
F. Central Coast
E. Sacramento−Delta
D. Sierra
C. Northeast
B. North Central
A. North Coast
50
45
40
35
30
25
20
15
10
5
1
Parker
Needles AP
50 Indio Fire
Brawley
Blythe
Fairmont
Death Valley
45 Redlands
Ojai
Cuyamaca
Tustin Irvine
Santa Barbara
40 Pasadena
Newport Beach
Chula Vista
Wasco
Tejon Rancho
35 Paso Robles
Merced AP
Lemon Cove
Hanford
Fresno WSO
30 Santa Cruz
San Luis Obispo
Berkeley
Vacaville
Petaluma
25 Napa
Marysville
Lodi
Livermore
Davis Exp Farm
20 Yosemite Park
Lake Spaulding
Electra PH
Colfax
Tahoe City
15 Susanville AP
Cedarville
Yreka
Willows 6W
Weaverville
10 Ukiah
Santa Rosa
Redding WSO
Orleans
Orland
5 Mount Shasta
Healdsburg
Chico Univ Farm
Fort Bragg 5N
1 Eureka WSO
1920
1930
1940
1950
1960
1970
1980
1990
2000

Figure 6a

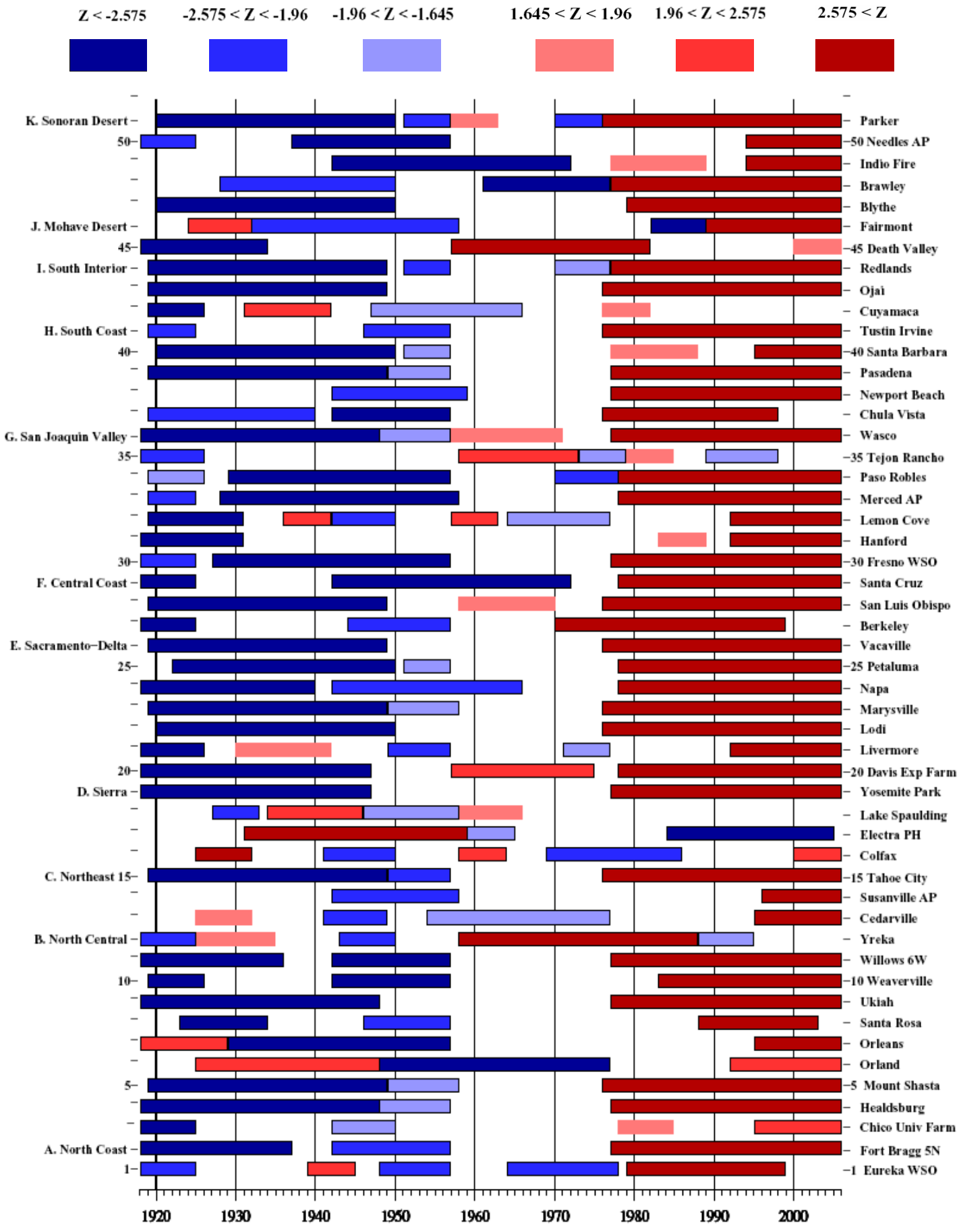
Z < -2.575
-2.575 < Z < -1.96
-1.96 < Z < -1.645
1.645 < Z < 1.96
1.96 < Z < 2.575
2.575 < Z
K. Sonoran Desert
50
J. Mohave Desert
45
I. South Interior
H. South Coast
40
G. San Joaquin Valley
35
F. Central Coast
E. Sacramento−Delta
25
D. Sierra
20
C. Northeast 15
B. North Central
10
A. North Coast
1
Parker
50 Needles AP
Indio Fire
Brawley
Blythe
Fairmont
45 Death Valley
Redlands
Ojai
Cuyamaca
Tustin Irvine
40 Santa Barbara
Pasadena
Newport Beach
Chula Vista
Wasco
35 Tejon Rancho
Paso Robles
Merced AP
Lemon Cove
Hanford
30 Fresno WSO
Santa Cruz
San Luis Obispo
Berkeley
Vacaville
25 Petaluma
Napa
Marysville
Lodi
Livermore
20 Davis Exp Farm
Yosemite Park
Lake Spaulding
Electra PH
Colfax
15 Tahoe City
Susanville AP
Cedarville
Yreka
Willows 6W
10 Weaverville
Ukiah
Santa Rosa
Orleans
Orland
5 Mount Shasta
Healdsburg
Chico Univ Farm
Fort Bragg 5N
1 Eureka WSO
1920
1930
1940
1950
1960
1970
1980
1990
2000

Figure 6b

USHCN Annual Tmax Trends (1918-2006)

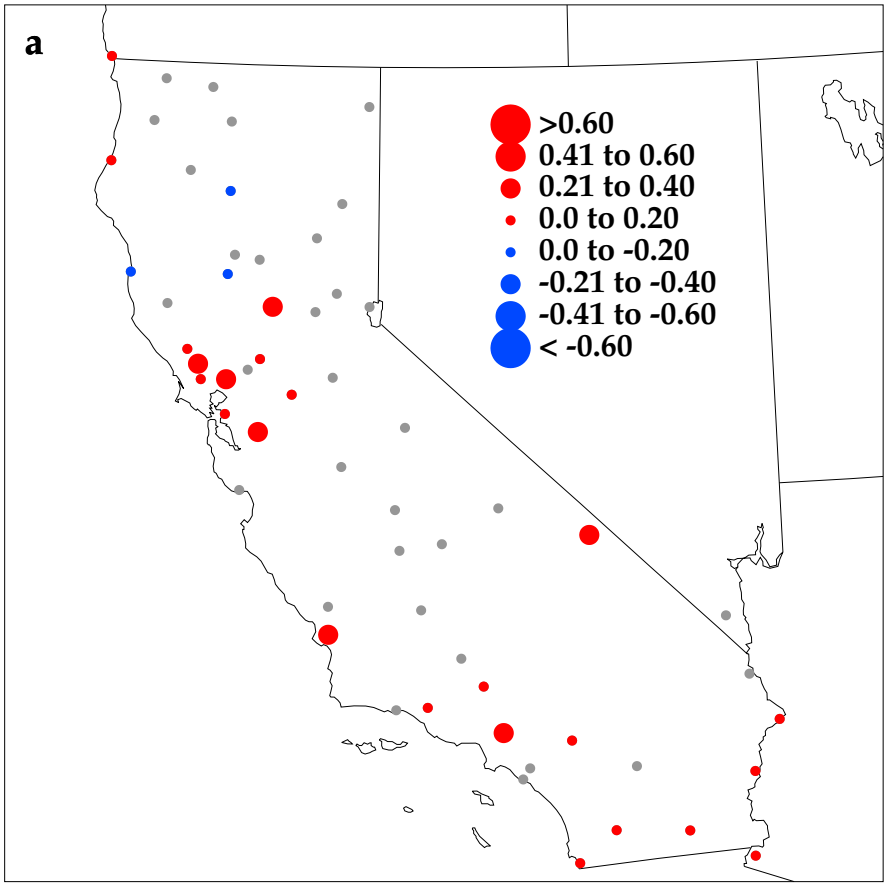

Warming Stations = 23

Cooling Stations = 3

USHCN Annual Tmin Trends (1918-2006)

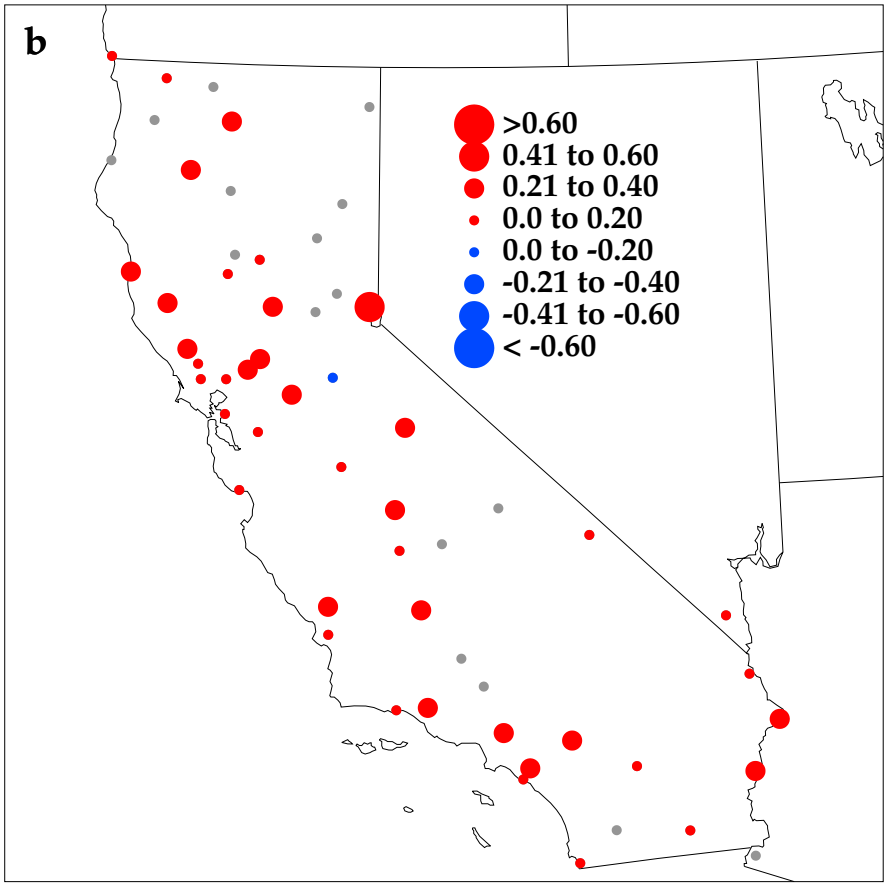

Warming Stations = 41

Cooling Stations = 1

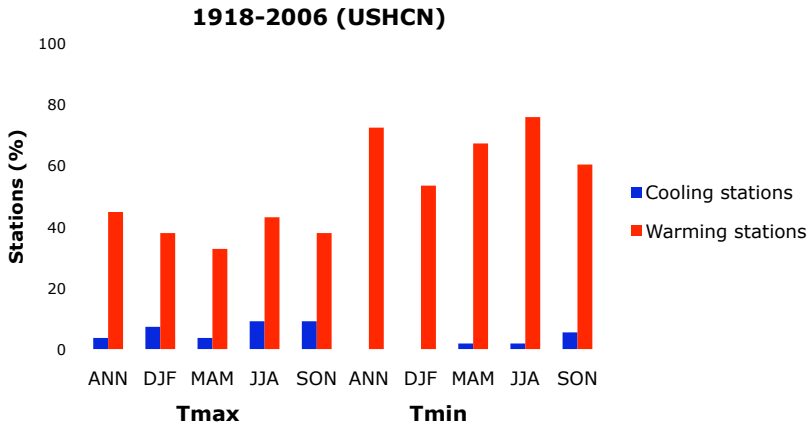
1918-2006 (USHCN)
Stations (%)
100
80
60
40
20
0
ANN DJF MAM JJA SON ANN DJF MAM JJA SON
Tmax
Tmin
Cooling stations
Warming stations

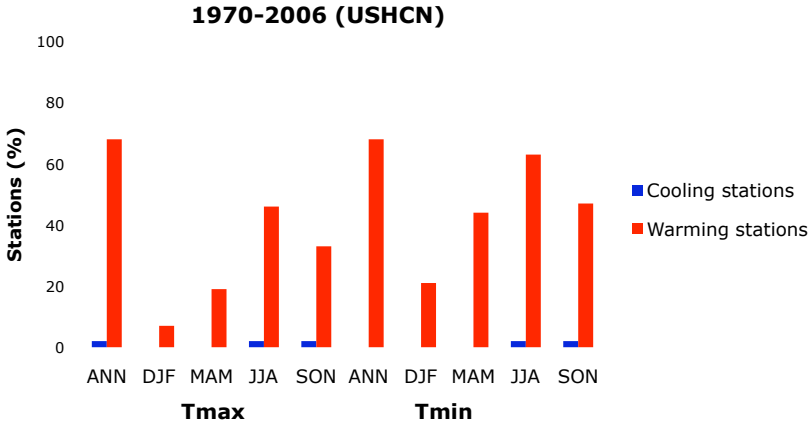
1970-2006 (USHCN)
Stations (%)
100
80
60
40
20
0
ANN DJF MAM JJA SON ANN DJF MAM JJA SON
Tmax
Tmin
Cooling stations
Warming stations

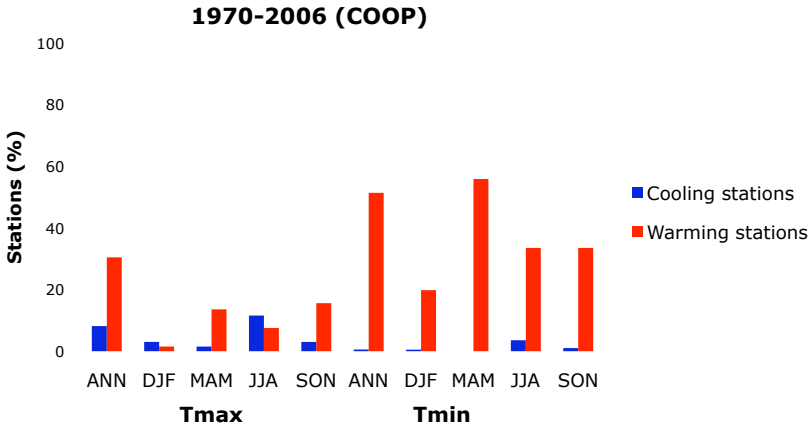
1970-2006 (COOP)
Stations (%)
100
80
60
40
20
0
ANN DJF MAM JJA SON ANN DJF MAM JJA SON
Tmax
Tmin
Cooling stations
Warming stations

Figure 8

USHCN Annual Tmax Trends (1970-2006)

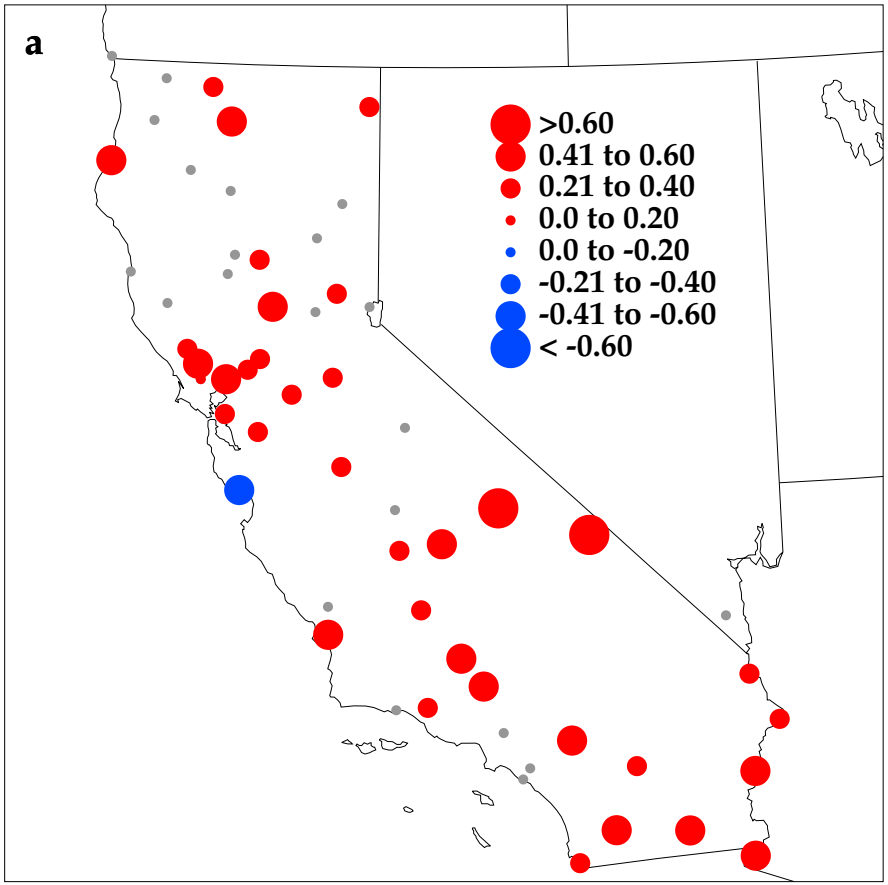

Warming Stations = 36

Cooling Stations = 1

USHCN Annual Tmin Trends (1970-2006)

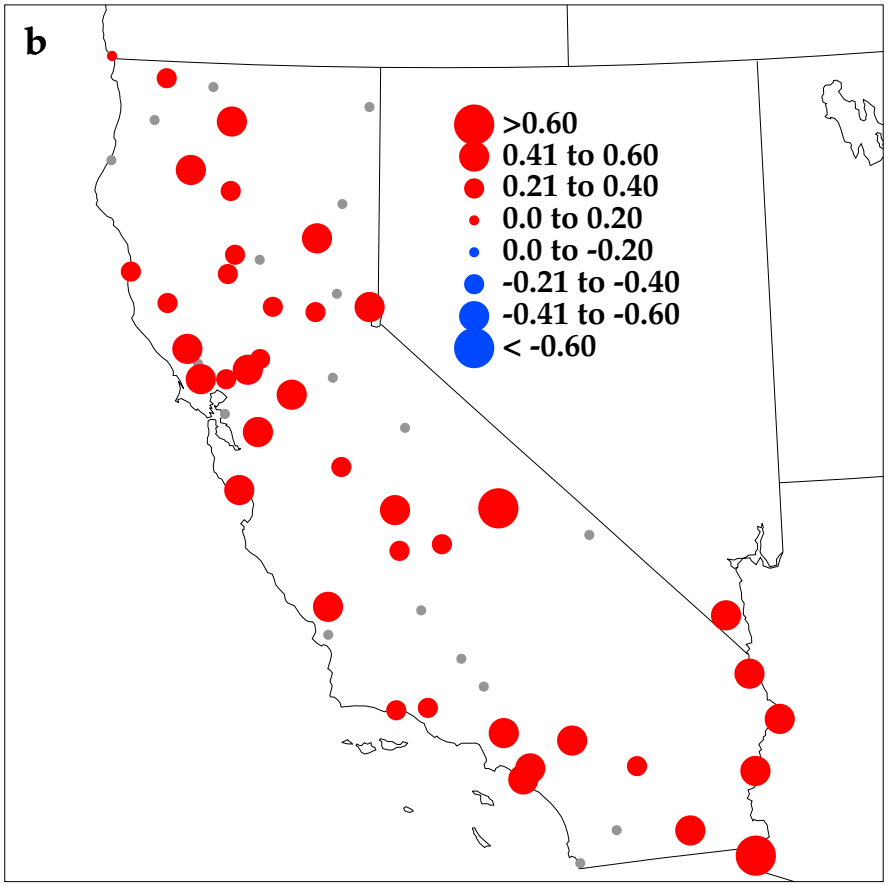

Warming Stations = 40

Cooling Stations = 0

COOP Annual Tmax Trends (1970-2006)

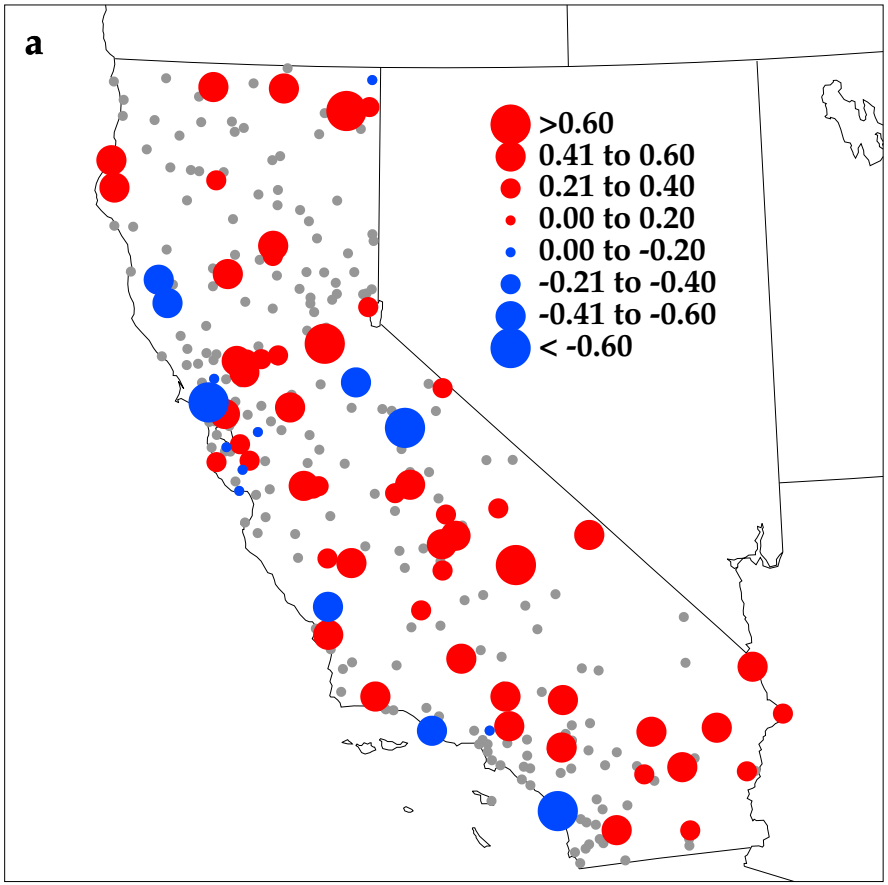

Warming Stations = 56

Cooling Stations = 15

COOP Annual Tmin Trends (1970-2006)

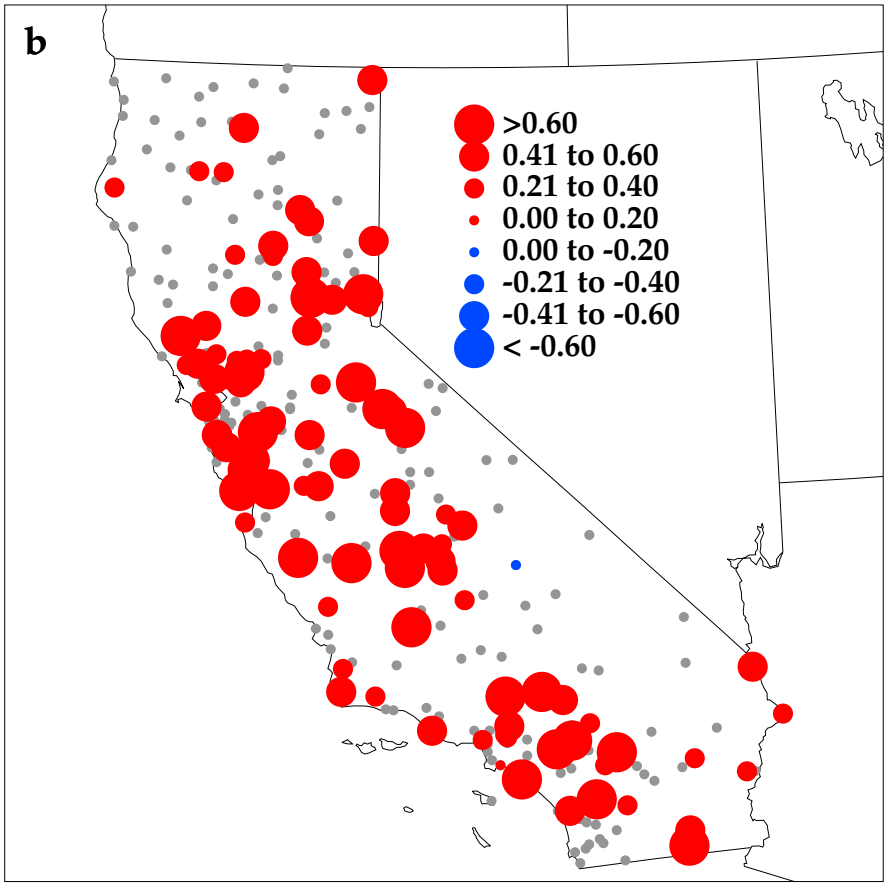

Warming Stations = 94

Cooling Stations = 1

COOP DJF Tmax Trends (1970-2006)

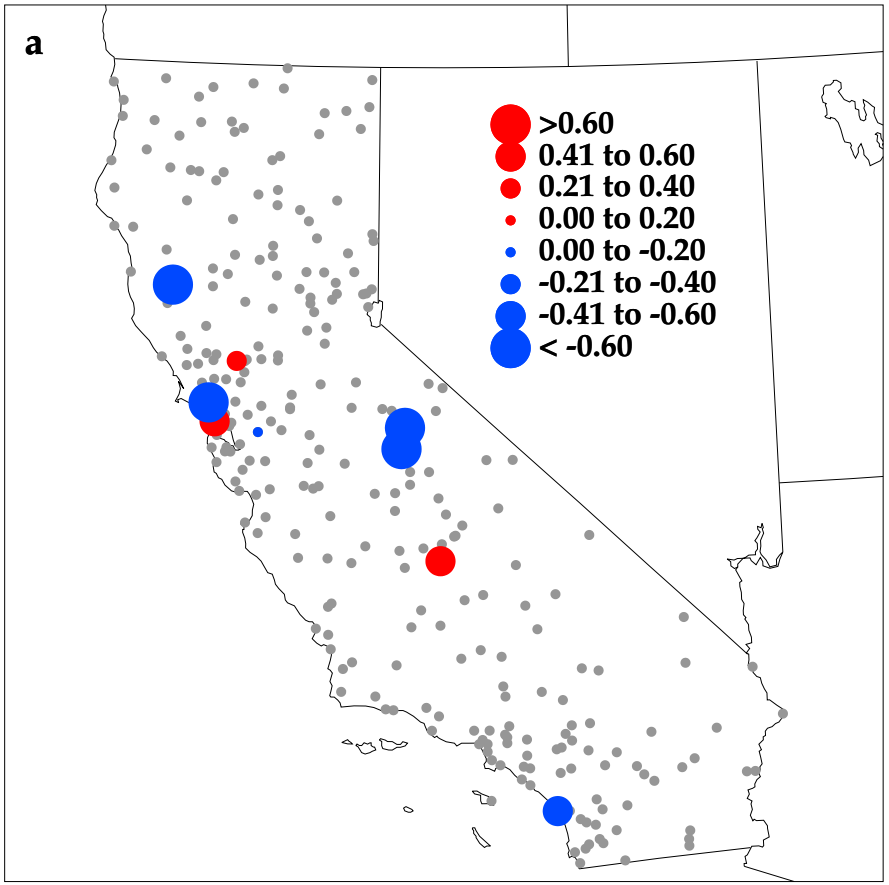

Warming Stations = 3

Cooling Stations = 6

COOP JJA Tmax Trends (1970-2006)

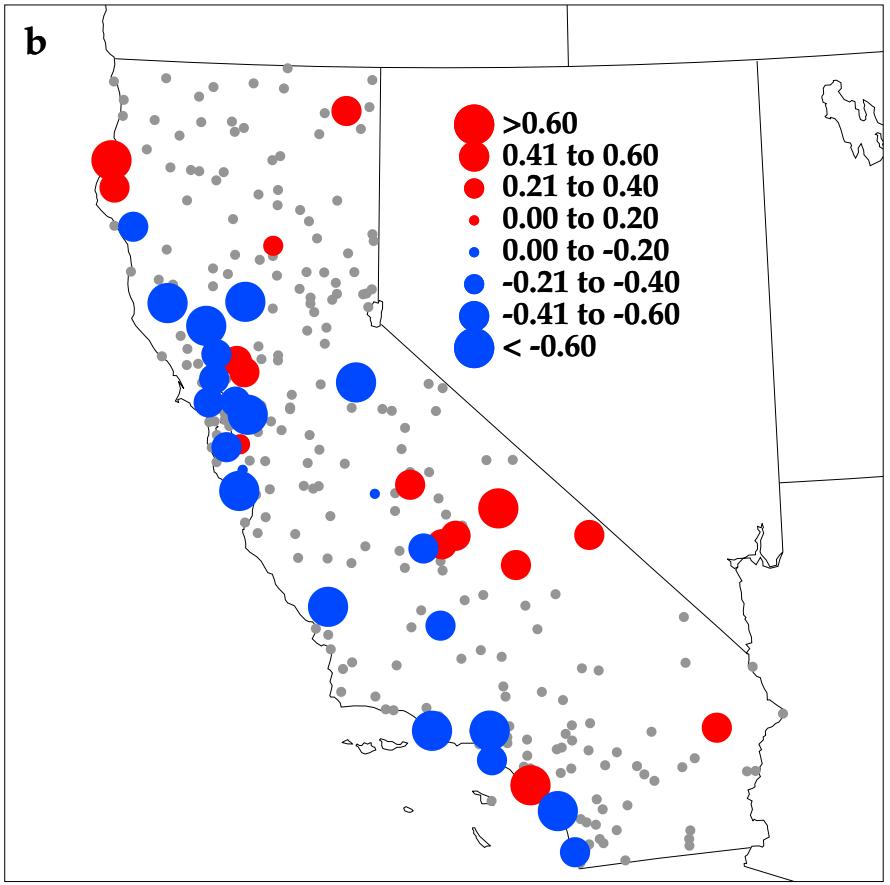

Warming Stations = 15

Cooling Stations = 23

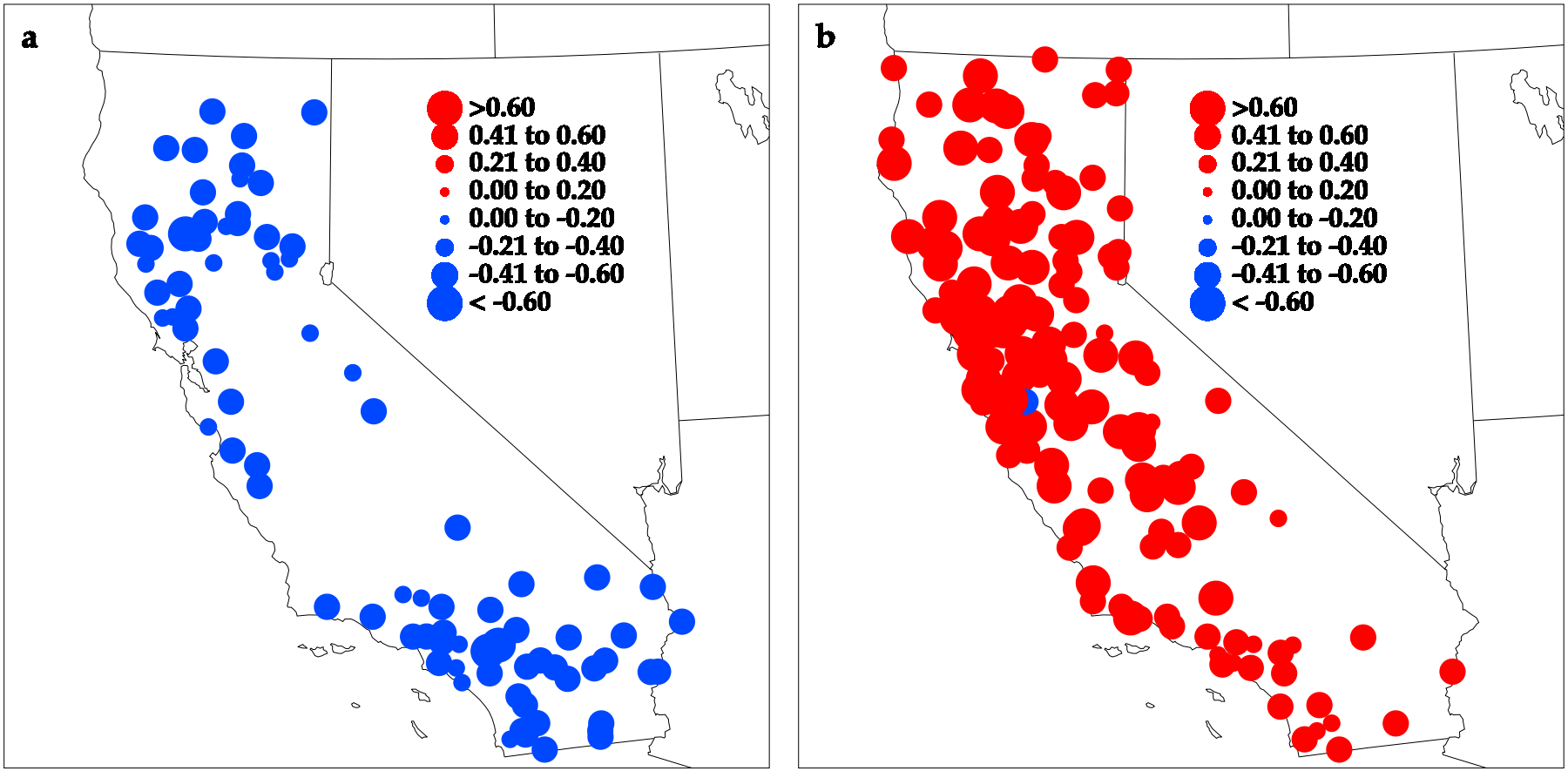
a
>0.60
0.41 to 0.60
0.21 to 0.40
0.00 to 0.20
0.00 to -0.20
-0.21 to -0.40
-0.41 to -0.60
< -0.60
b
>0.60
0.41 to 0.60
0.21 to 0.40
0.00 to 0.20
0.00 to -0.20
-0.21 to -0.40
-0.41 to -0.60
< -0.60